

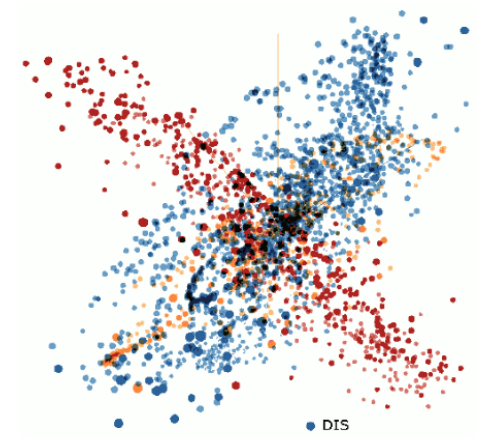
# The HEP implications of an EIC

a theory/PDF analysis perspective.

Tim Hobbs, CTEQ@SMU and JLab EIC Center

July 25<sup>th</sup> 2019

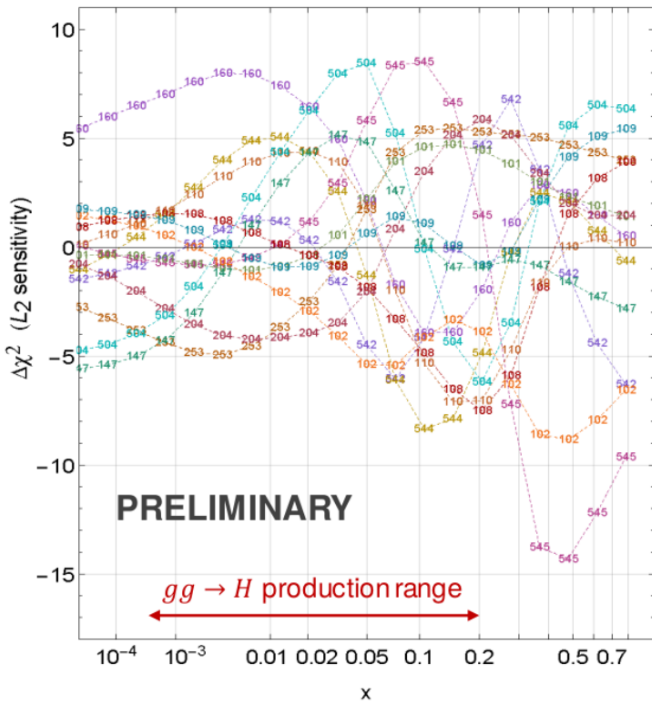
Collaboration with Bo-Ting Wang, Pavel Nadolsky, Fred Olness  
...and CTEQ-TEA, EIC<sup>2</sup>@JLab...



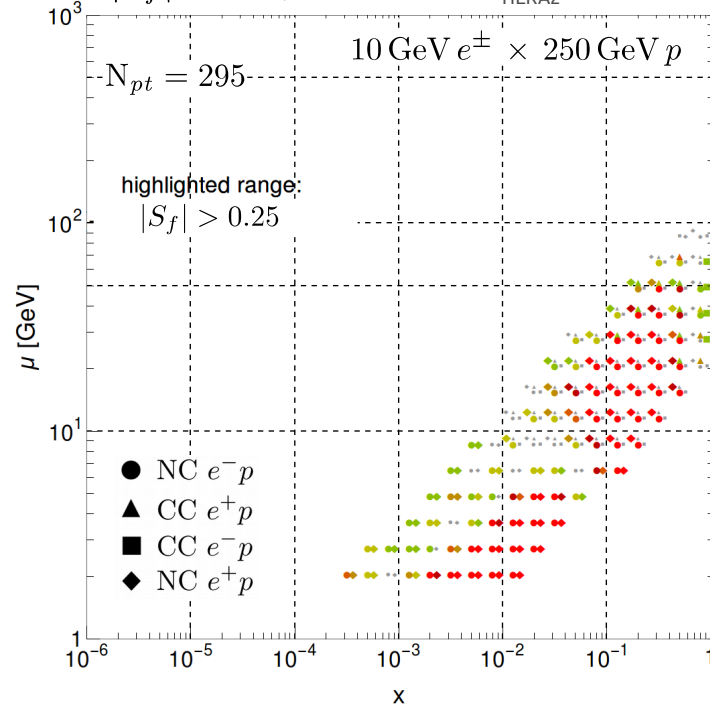
DIS  
VBP  
Jets, tT



CT18 NNLO,  $g(x, 100 \text{ GeV})$



$|S_f|$  for  $\sigma_H$ , 14 TeV CT14<sub>HERA2</sub> NNLO

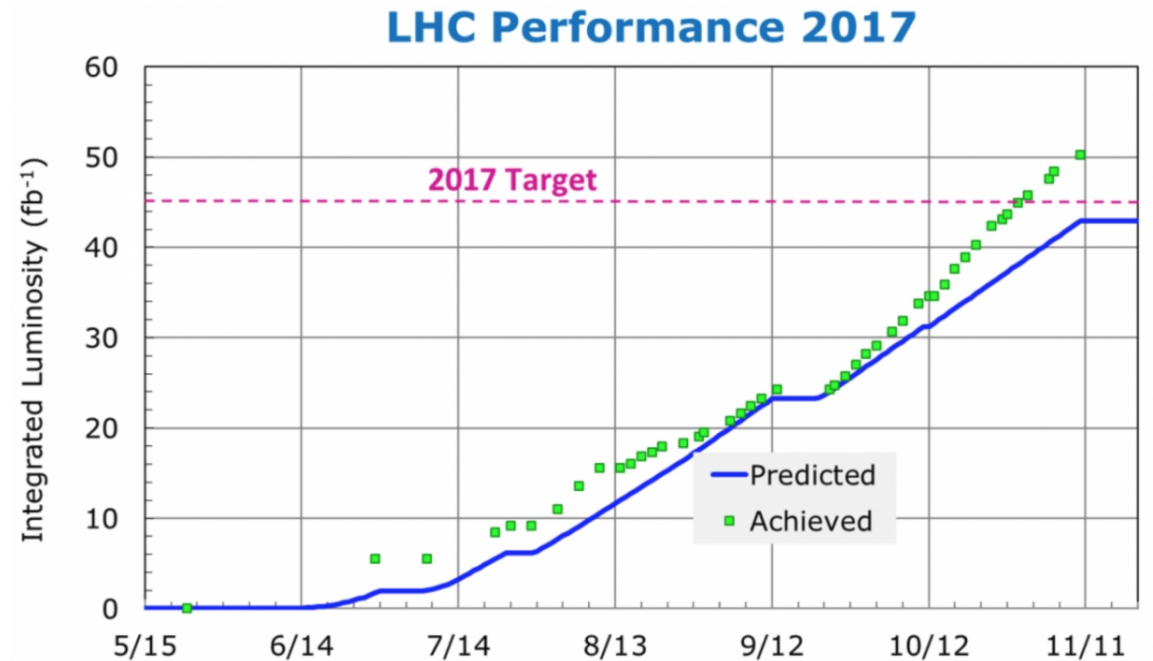


EIC User Group Meeting '19. Paris; 22-26 July 2019.



# the view from particle phenomenology

- with the completion of Run-2, LHC has accumulated copious data



- this data is an opportunity, but also a challenge:

→ many standard-candle measurements are crucially limited by PDF uncertainties, as are new physics searches

(See talk by Paul Newman, 22 July.)

e.g.,  $\sigma_H$ ,  $\sin^2 \theta_W$ ,  $M_W$ , ...

→ to reach (sub)percent-level precision objectives for HL-LHC, PDF improvements are obligatory; must resolve tensions/pulls in modern PDF analyses

→ input from EIC will be essential

- there remains considerable dependence (as large as  $\sim 13\%$ ) upon PDF parametrization and running coupling

→ the situation is such that precision in Higgs phenom. is significantly **PDF-limited**

Accardi et al., EPJC76, 471 (2016).

PDF sets	$\sigma(H)^{\text{NNLO}}$ (pb) nominal $\alpha_s(M_Z)$	$\sigma(H)^{\text{NNLO}}$ (pb) $\alpha_s(M_Z) = 0.115$	$\sigma(H)^{\text{NNLO}}$ (pb) $\alpha_s(M_Z) = 0.118$
ABM12 [2]	$39.80 \pm 0.84$	$41.62 \pm 0.46$	$44.70 \pm 0.50$
CJ15 [1] <sup>a</sup>	$42.45^{+0.43}_{-0.18}$	$39.48^{+0.40}_{-0.17}$	$42.45^{+0.43}_{-0.18}$
CT14 [3] <sup>b</sup>	$42.33^{+1.43}_{-1.68}$	$39.41^{+1.33}_{-1.56}$ (40.10)	$42.33^{+1.43}_{-1.68}$
HERAPDF2.0 [4] <sup>c</sup>	$42.62^{+0.35}_{-0.43}$	$39.68^{+0.32}_{-0.40}$ (40.88)	$42.62^{+0.35}_{-0.43}$
JR14 (dyn) [5]	$38.01 \pm 0.34$	$39.34 \pm 0.22$	$42.25 \pm 0.24$
MMHT14 [6]	$42.36^{+0.56}_{-0.78}$	$39.43^{+0.53}_{-0.73}$ (40.48)	$42.36^{+0.56}_{-0.78}$
NNPDF3.0 [7]	$42.59 \pm 0.80$	$39.65 \pm 0.74$ (40.74 $\pm$ 0.88)	$42.59 \pm 0.80$
PDF4LHC15 [8]	$42.42 \pm 0.78$	$39.49 \pm 0.73$	$42.42 \pm 0.78$

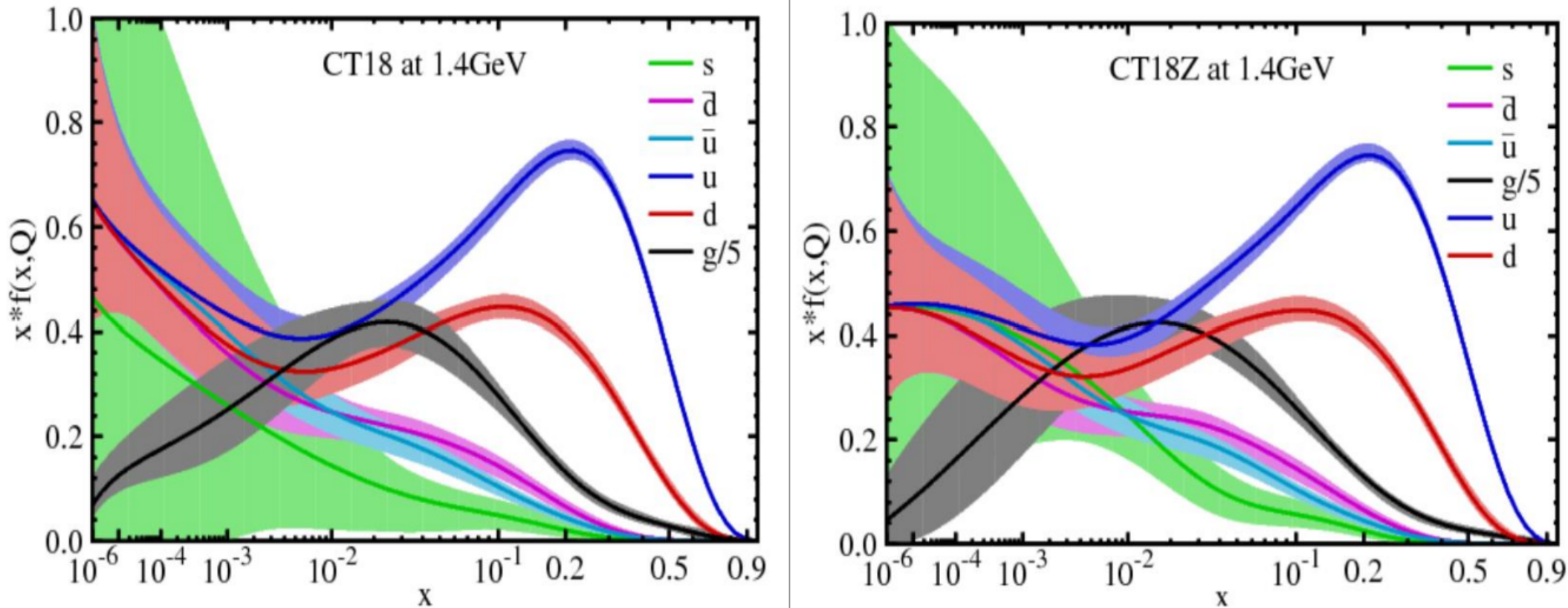
$\sigma_H$  at NNLO and  $\sqrt{s} = 13 \text{ TeV}$ ;  $\mu_F = \mu_R = m_H$

→ enhancing the discovery potential in the Higgs sector will require improving these uncertainties!

# CT18 parton distributions

PDF analyses are challenging! (theoretically, computationally, statistically, ... )

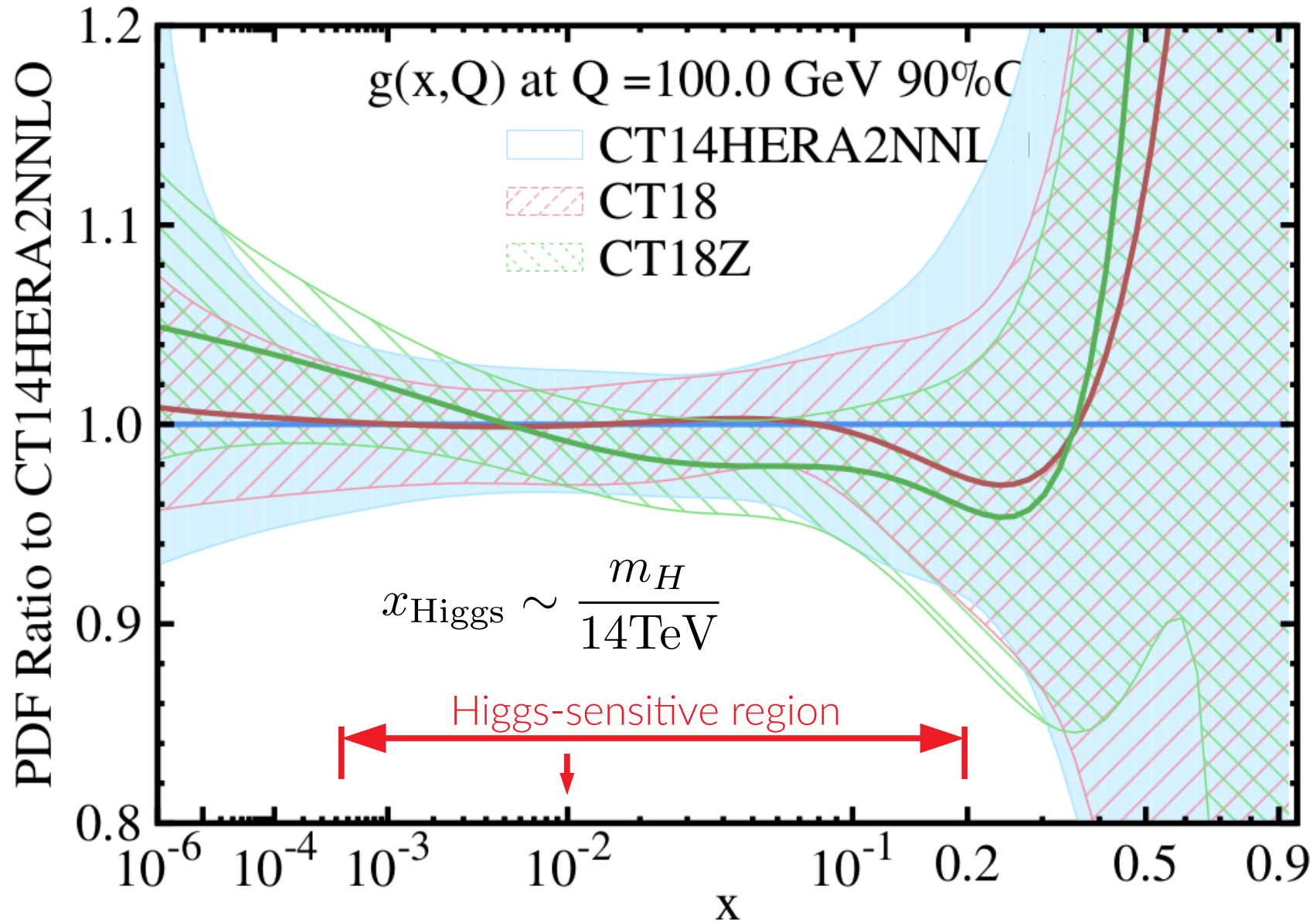
## Four PDF ensembles: CT18 (default), A, X, and Z



CT18Z has enhanced gluon and strange PDFs at  $x \sim 10^{-4}$ , and reduced light-quark PDFs at  $x < 10^{-2}$ . The CT18Z fit is performed so as to maximize the differences from CT18 PDFs, while preserving about the same goodness-of-fit as for CT18. CT18A and CT18X include some features of CT18Z

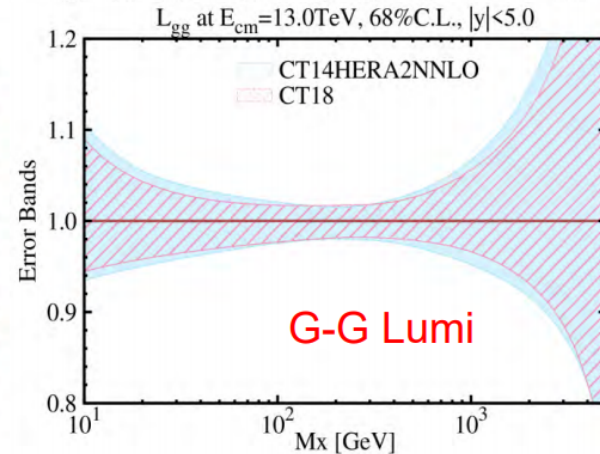
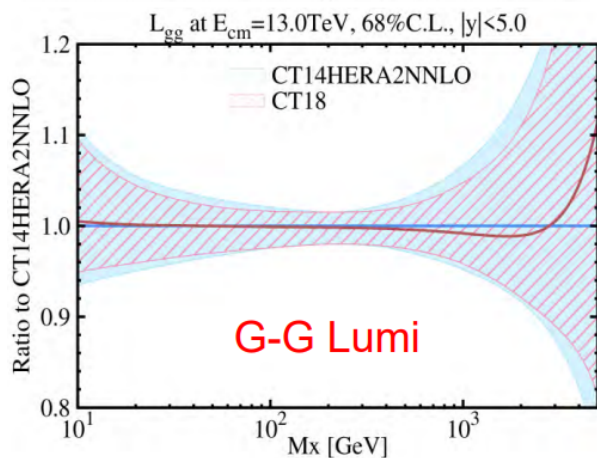
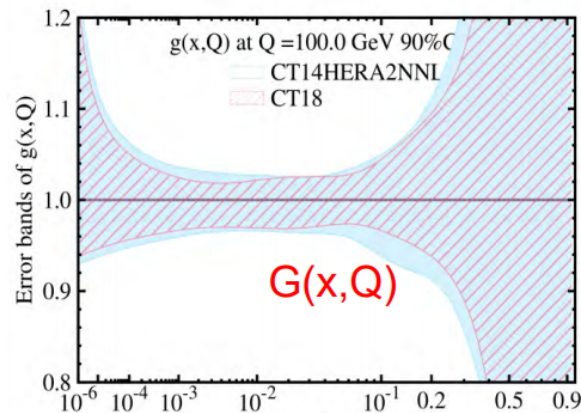
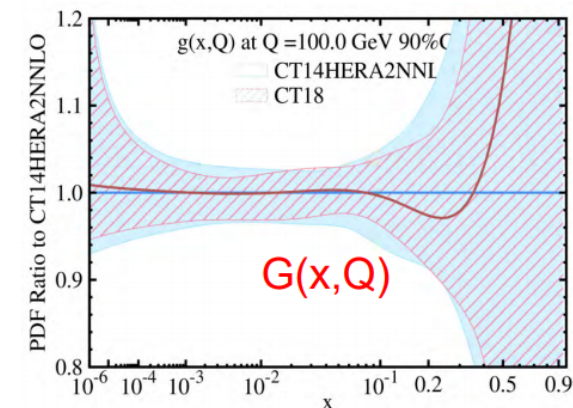
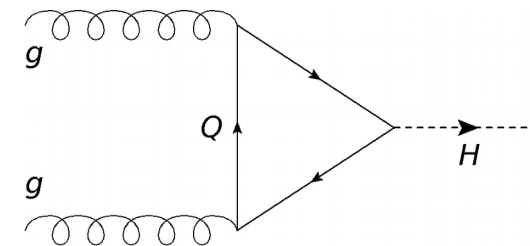


# LHC Run-1 gluon PDF impact in CT14 $\rightarrow$ CT18(Z)



- while LHC Run-1 data drive important PDF improvements, including for the gluon at high-, low- $x$ , the effect is relatively incremental

CT14  $\rightarrow$  CT18 modestly shifts Higgs cross sections and slightly reduces PDF uncertainties



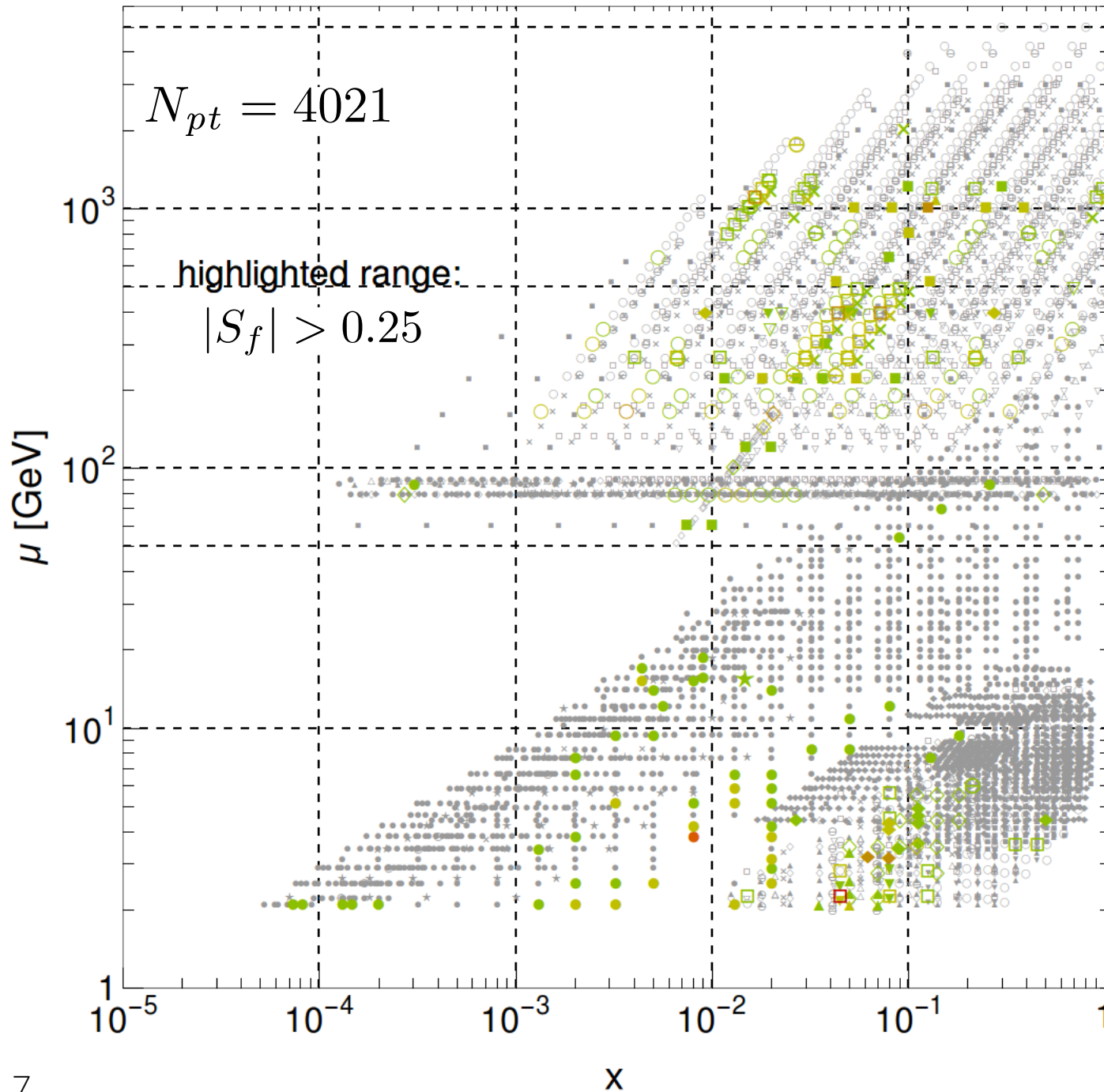
7 TeV		
	$\sigma(\text{gg-h})$	$\delta\sigma \text{ sym}(90\% \text{C.L.})$
CT14NNLO	14.67	0.46
CT18	14.57	0.44
8 TeV		
	$\sigma(\text{gg-h})$	$\delta\sigma \text{ sym}(90\% \text{C.L.})$
CT14NNLO	18.70	0.57
CT18	18.45	0.55
13 TeV		
	$\sigma(\text{gg-h})$	$\delta\sigma \text{ sym}(90\% \text{C.L.})$
CT14NNLO	42.78	1.32
CT18	42.43	1.26
14 TeV		
	$\sigma(\text{gg-h})$	$\delta\sigma \text{ sym}(90\% \text{C.L.})$
CT14NNLO	48.23	1.50
CT18	47.91	1.42

PDF induced errors (at 90% CL) are reduced by about 5% as compared to CT14 predictions.

$\rightarrow$  can we disentangle elements of the global analysis responsible for these improvements?

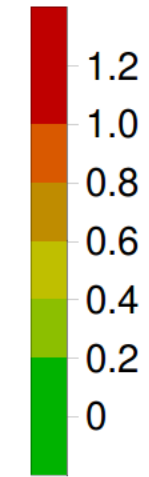
# $|S_f|$ for $\sigma_{H^0}$ 14 TeV, CT14<sub>HERA2</sub> NNLO

B.-T. Wang, TJH, S. Doyle, J. Gao, T.-J. Hou, P. M. Nadolsky, F. I. Olness  
[Phys.Rev. D98 \(2018\) 094030](#)



(magnitude of PDF pull of each datum)

$|S_f|$



• after the aggregated HERA data, inclusive jet production – greatest total sensitivity!

→ large correlations for E866, BCDMS, CCFR, CMS WASY, Z  $p_T$  and  $t\bar{t}$  production, but smaller numbers of highly-sensitive points



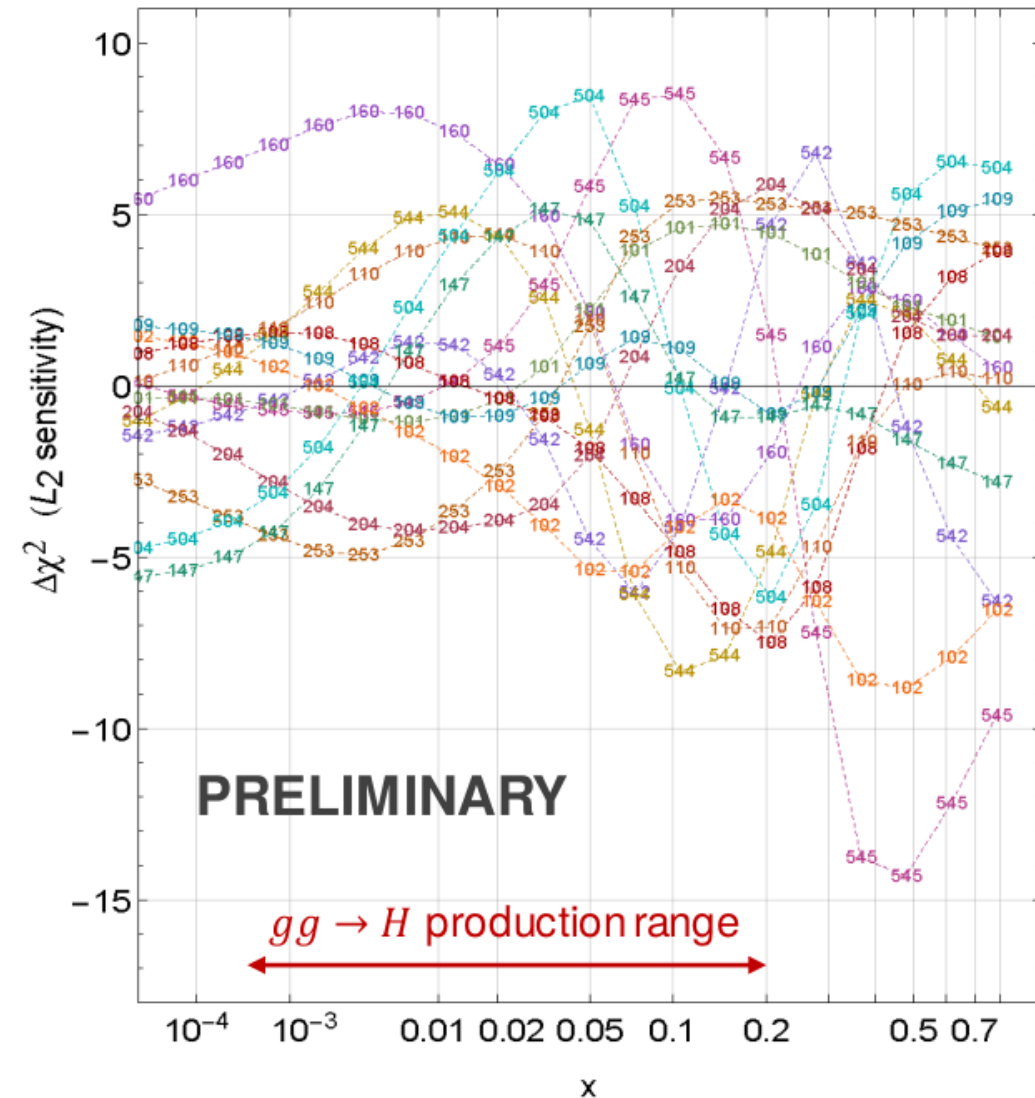


# Estimated $\chi^2$ pulls from experiments

( $L_2$  sensitivity, arXiv:1904.00222, v. 2)

CT18 NNLO,  $g(x, 100 \text{ GeV})$

CT18 NNLO, gluon at  $Q=100 \text{ GeV}$



Most sensitive experiments

- 253--- ATL8ZpTbT
- 542--- CMS7jtR7y6T
- 544--- ATL7jtR6uT
- 545--- CMS8jtR7T
- 160--- HERAplI
- 101--- BcdF2pCor
- 102--- BcdF2dCor
- 108--- cdhswf2
- 109--- cdhswf3
- 110--- ccfrf2.mi
- 147--- Hn1X0c
- 204--- e866ppxf
- 504--- cdf2jtCor2

↑ stronger  
(anti-) correlation  
↓

Experiments with large  $\Delta\chi^2 > 0$  [ $\Delta\chi^2 < 0$ ] pull  $g(x, Q)$  in the negative [positive] direction at the shown  $x$

Estimated using CT18 Hessian PDFs

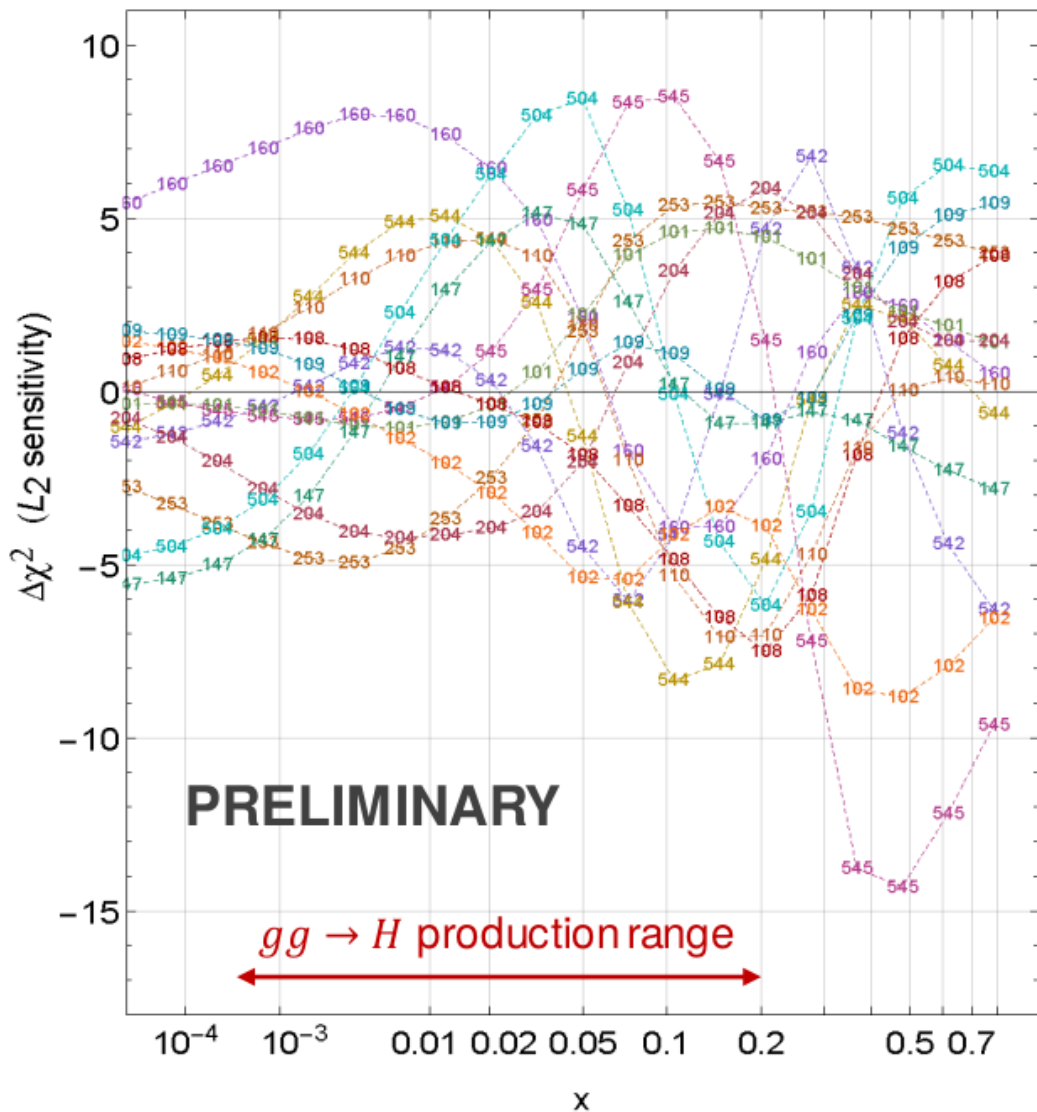
$$S_{f, L_2} \sim \text{Corr}[f_a, \chi_E^2]$$



# Estimated $\chi^2$ pulls from experiments

( $L_2$  sensitivity, arXiv:1904.00222, v. 2)

CT18 NNLO,  $g(x, 100 \text{ GeV})$



precise data from EIC sensitive to the gluon PDF Higgs region needed to help unravel the systematic tensions evident here

## Most sensitive experiments

- 253--- ATLAS8ZpTbT
- 542--- CMS7jtR7y6T
- 544--- ATLAS7jtR6uT
- 545--- CMS8jtR7T
- 160--- HERAIpII
- 101--- BcdF2pCor
- 102--- BcdF2dCor
- 108--- cdhswf2
- 109--- cdhswf3
- 110--- ccrf2.mi
- 147--- Hn1X0c
- 204--- e866ppxf
- 504--- cdf2jtCor2



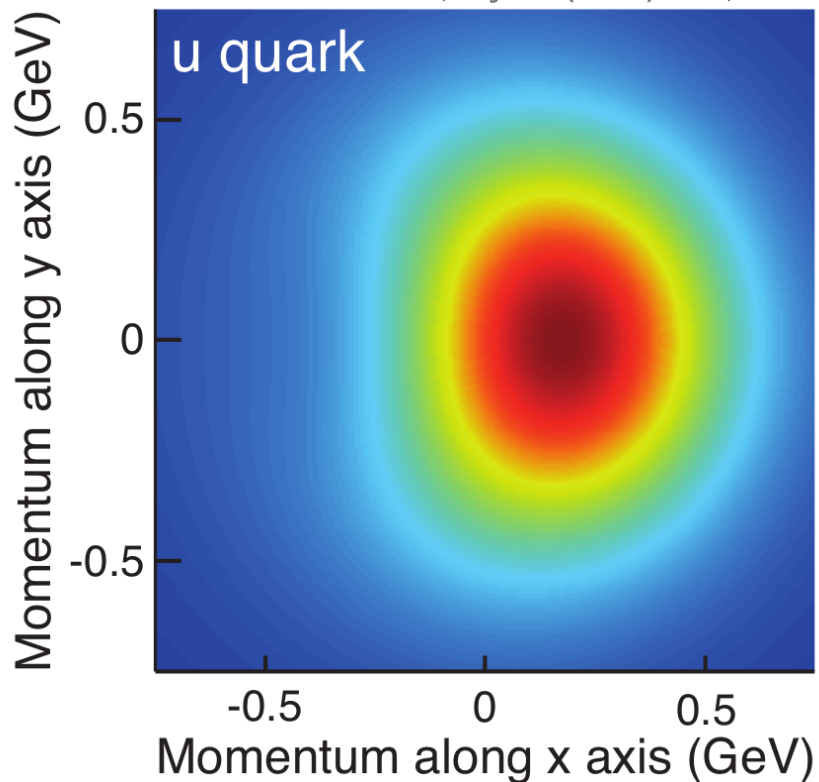
Note opposite pulls (tensions) in some  $x$  ranges between HERA I+II DIS (ID=160); CDF (504), ATLAS 7 (544), CMS 7 (542), CMS 8 jet (545) production; E866pp DY (204); ATLAS 8 Z pT (253) production; BCDMS and CDHSW DIS

$$S_{f,L_2} \sim \text{Corr}[f_a, \chi_E^2]$$

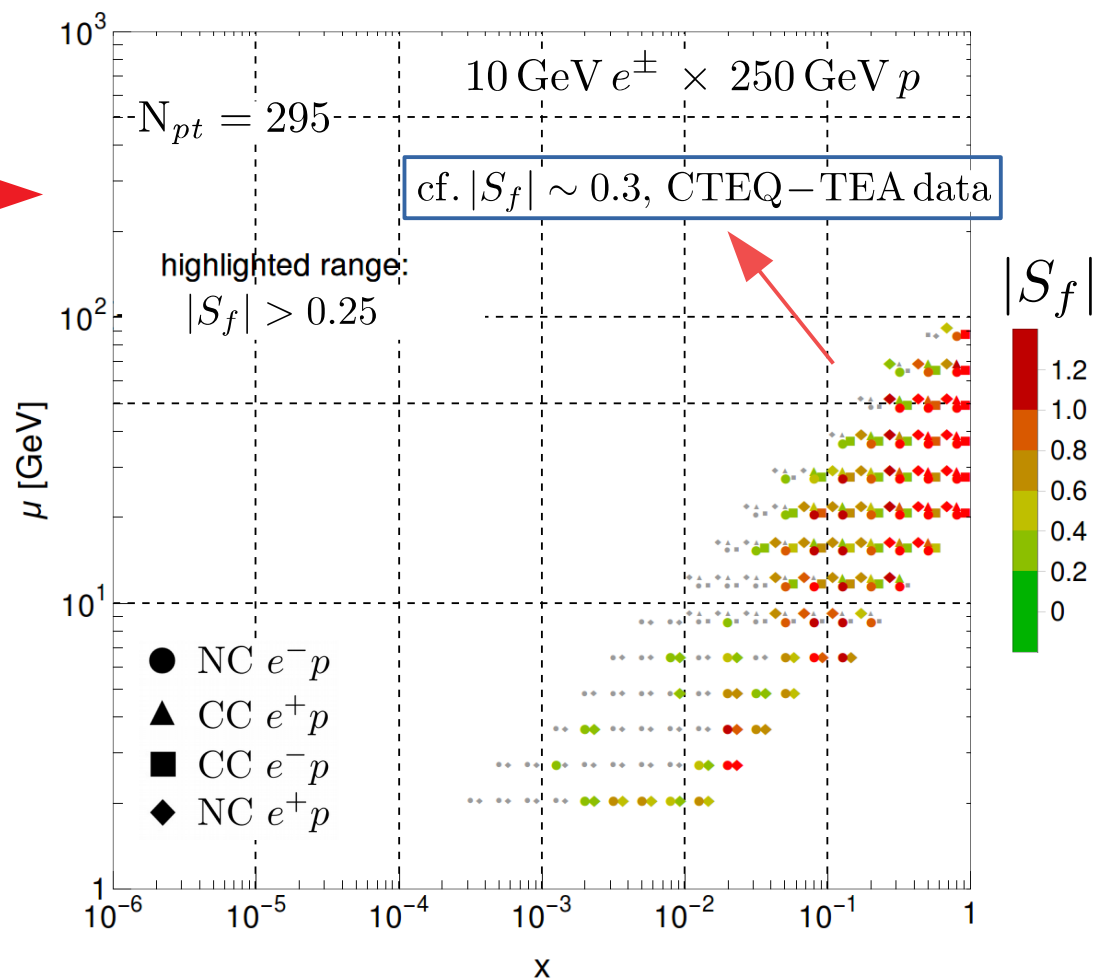
# the EIC tomography program will deliver high-precision DIS

- by measuring the nucleon's multi-dimensional wave function with high precision, the EIC will hugely constrain proton collinear structure

Accardi et al., EPJA52 (2016) no.9, 268.

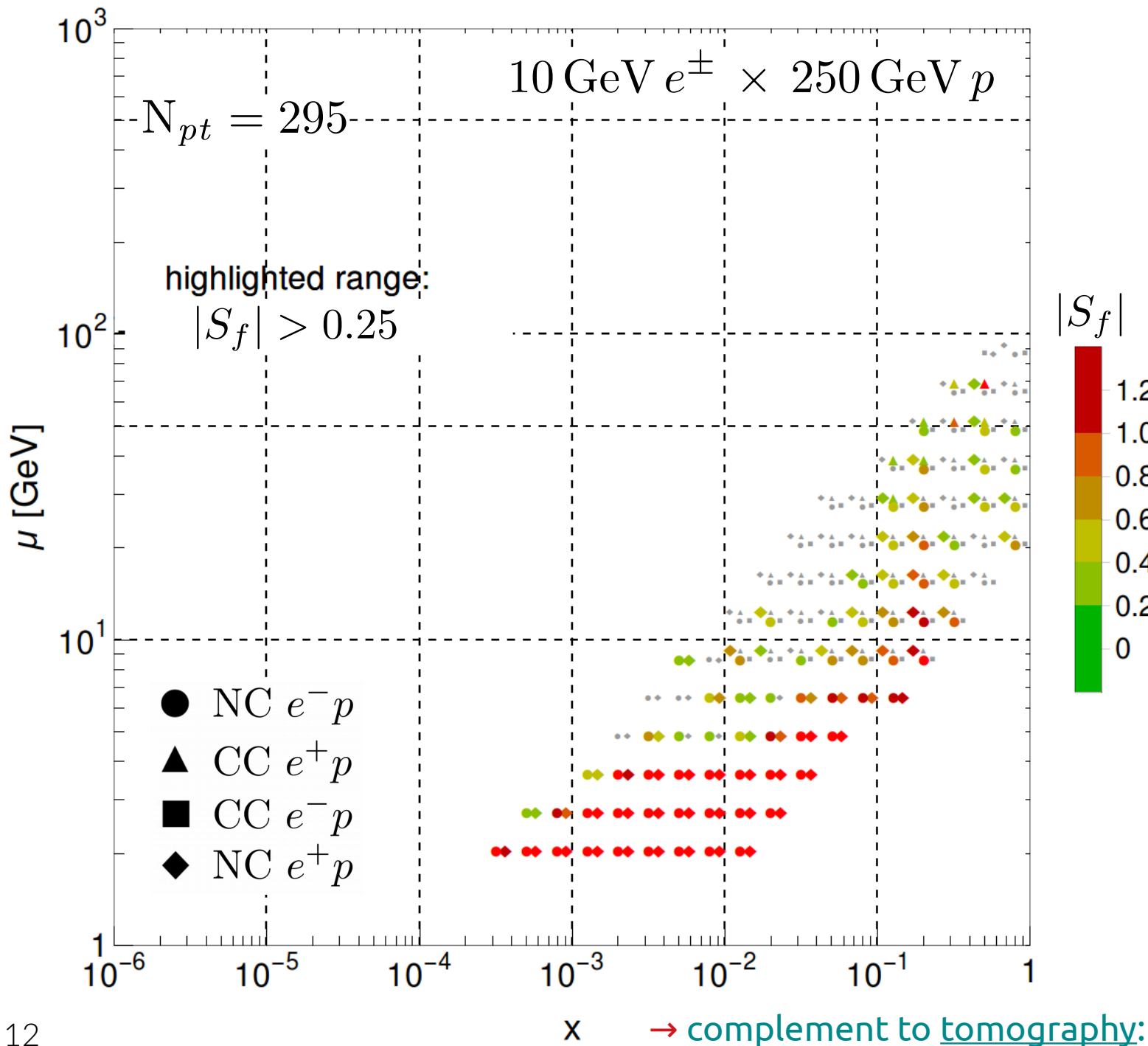


$|S_f|$  for  $d/u(x, \mu)$ , CT14<sub>HERA2</sub> NNLO



- DIS cross sections from EIC will supercede the bulk of fixed-target information in contemporary QCD fits; provide an 'anchor-point' to resolve systematic PDF tensions

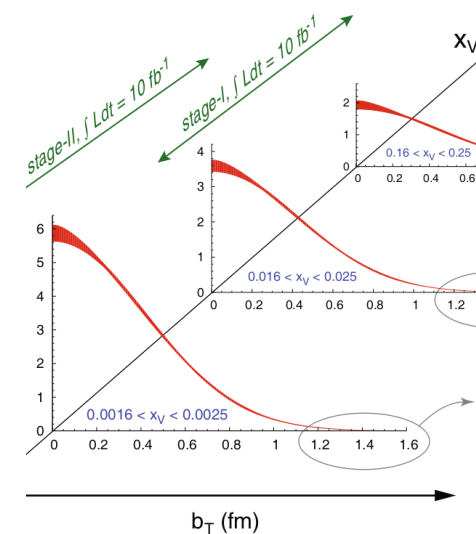
# $|S_f|$ for $g(x, \mu)$ CT14 HERA2 NNLO



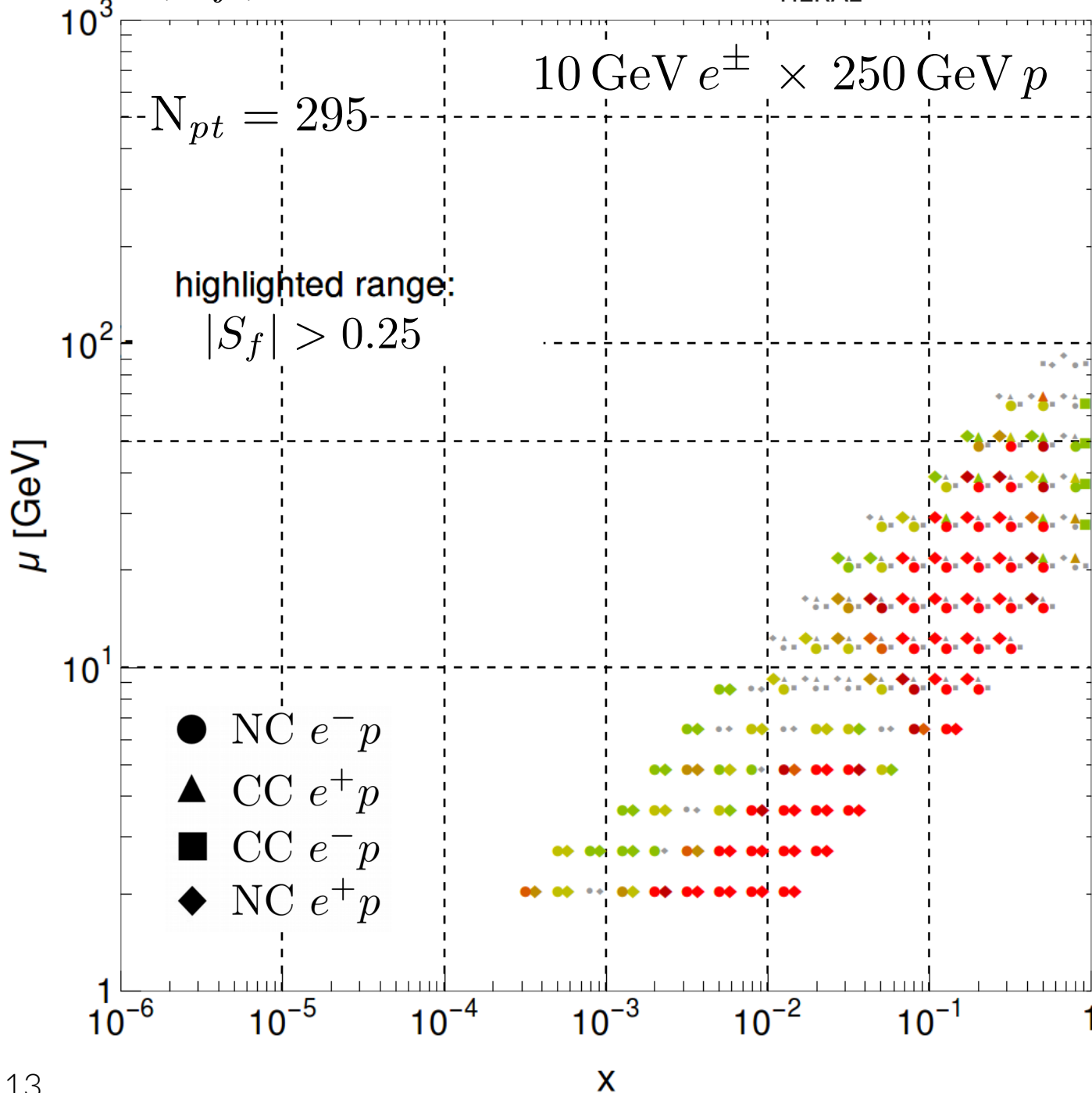
- an EIC will provide a sensitive probe to the gluon distribution – especially at low  $x$

$$x \gtrsim 3 \times 10^{-4}$$

- these constraints arise from high statistics neutral current data on  $\sigma_{r,NC}^{e^\pm p}$

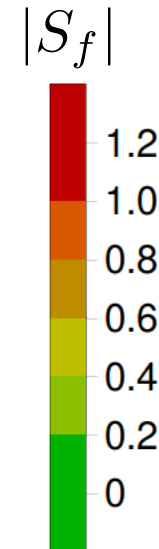


$|S_f|$  for  $\sigma_H$ , 14 TeV CT14<sub>HERA2</sub> NNLO

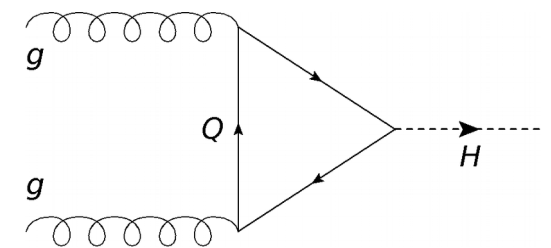


**potentially strong impact on the Higgs sector**

- the impact of an EIC upon the theoretical predictions for inclusive Higgs production arises from a very broad region of the kinematical space it can access



- impact rather closely tied to that of the integrated gluon PDF:

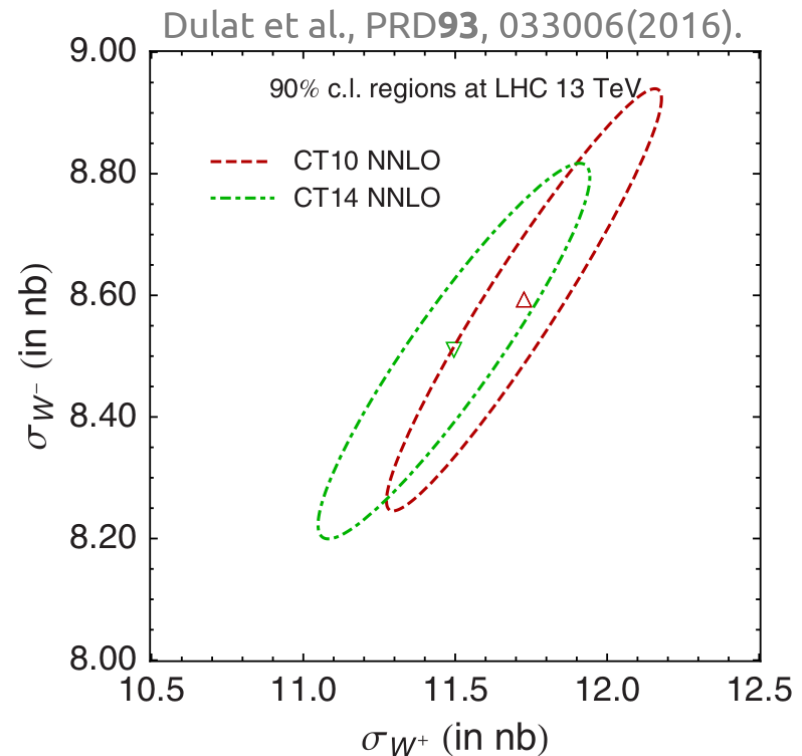
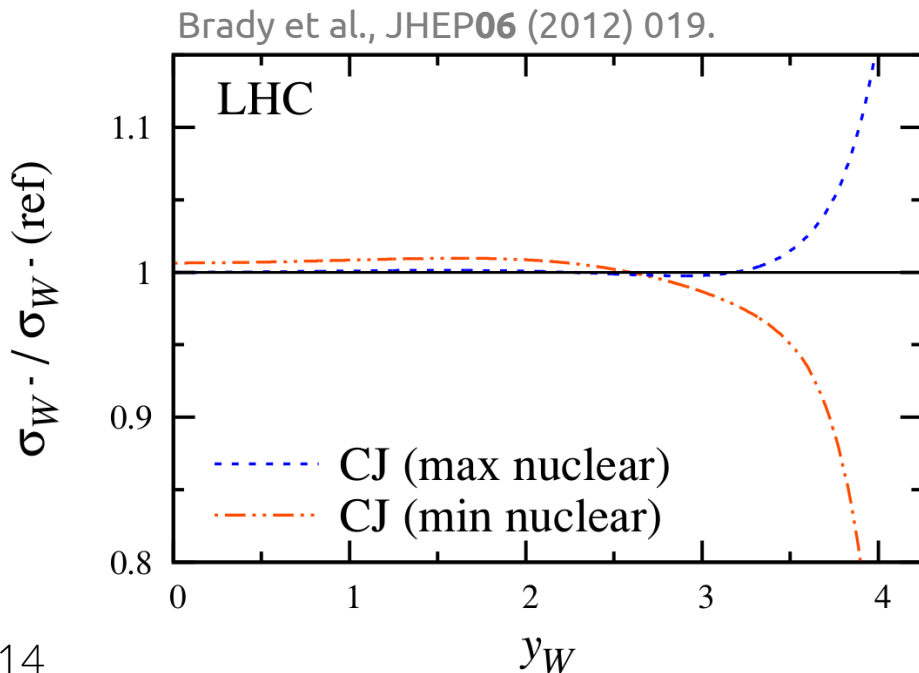


# EIC and an era of (higher) precision **electroweak physics** (?)

- theory predictions for the production of gauge bosons are quite sensitive to the nucleon PDFs: *e.g.*,  $d(x)$  at  $x \sim 1$ , which is poorly constrained

$$x_{1,2} = \frac{M}{\sqrt{s}} e^{\pm y}$$

$$\frac{d\sigma}{dy}(pp \rightarrow W^- X) = \frac{2\pi G_F}{3\sqrt{2}} x_1 x_2 \left( \cos^2 \theta_C \{d(x_1)\bar{u}(x_2) + \bar{u}(x_1)d(x_2)\} + \sin^2 \theta_C \{s(x_1)\bar{u}(x_2) + \bar{u}(x_1)s(x_2)\} \right)$$





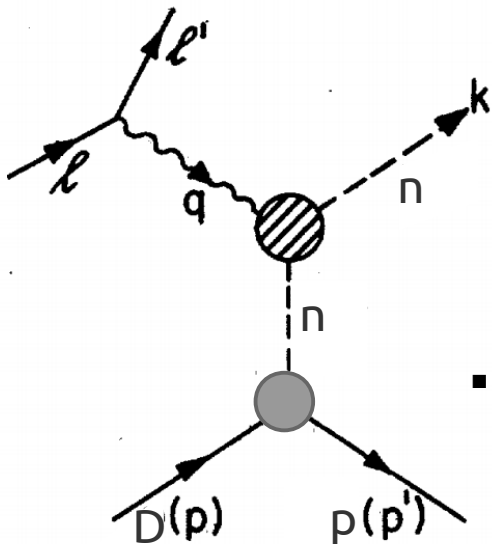
# historically, extractions of $d(x)$ , $x \rightarrow 1$ have depended on nuclear targets (and corrections!)

- in principle, a neutron target would allow the flavor separation needed to access  $d(x, Q^2)$

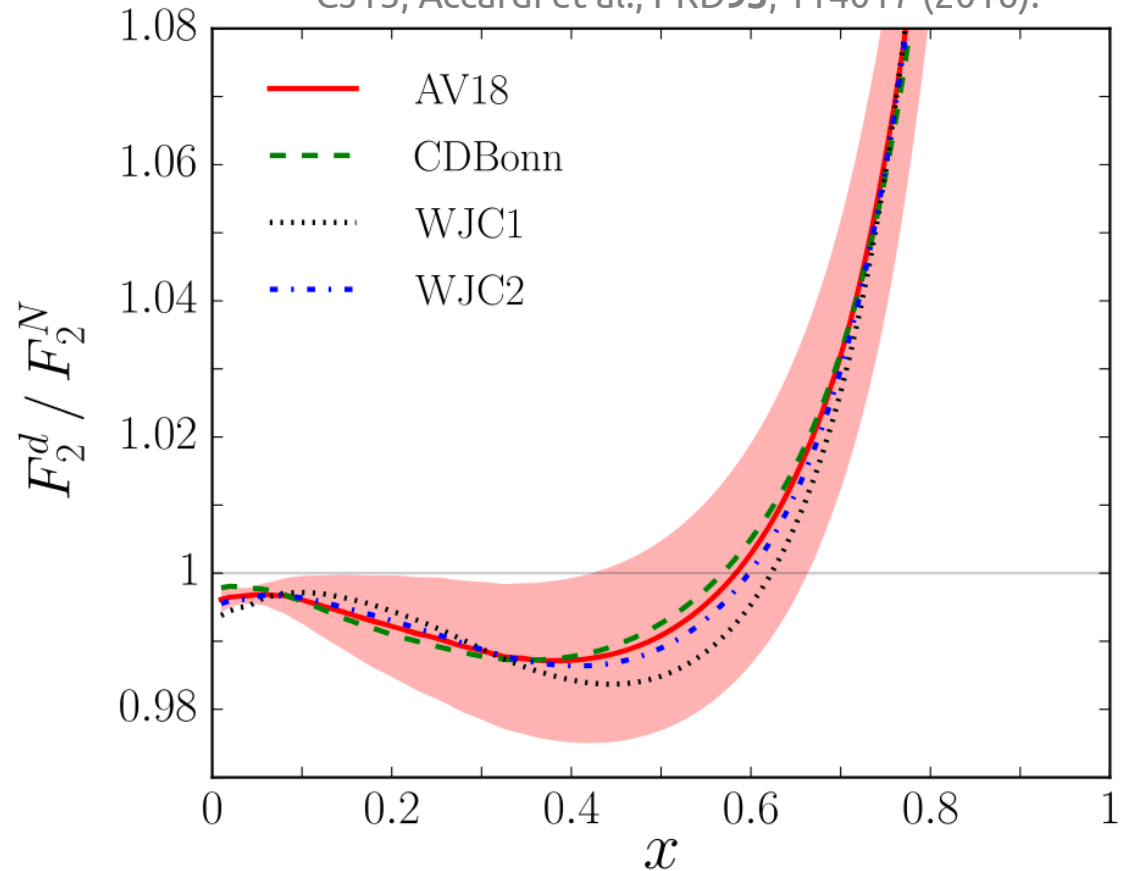
$$F_2^{e^- n} \sim x(4d + u)/9$$

— *vs* —

$$F_2^{e^- p} \sim x(4u + d)/9$$



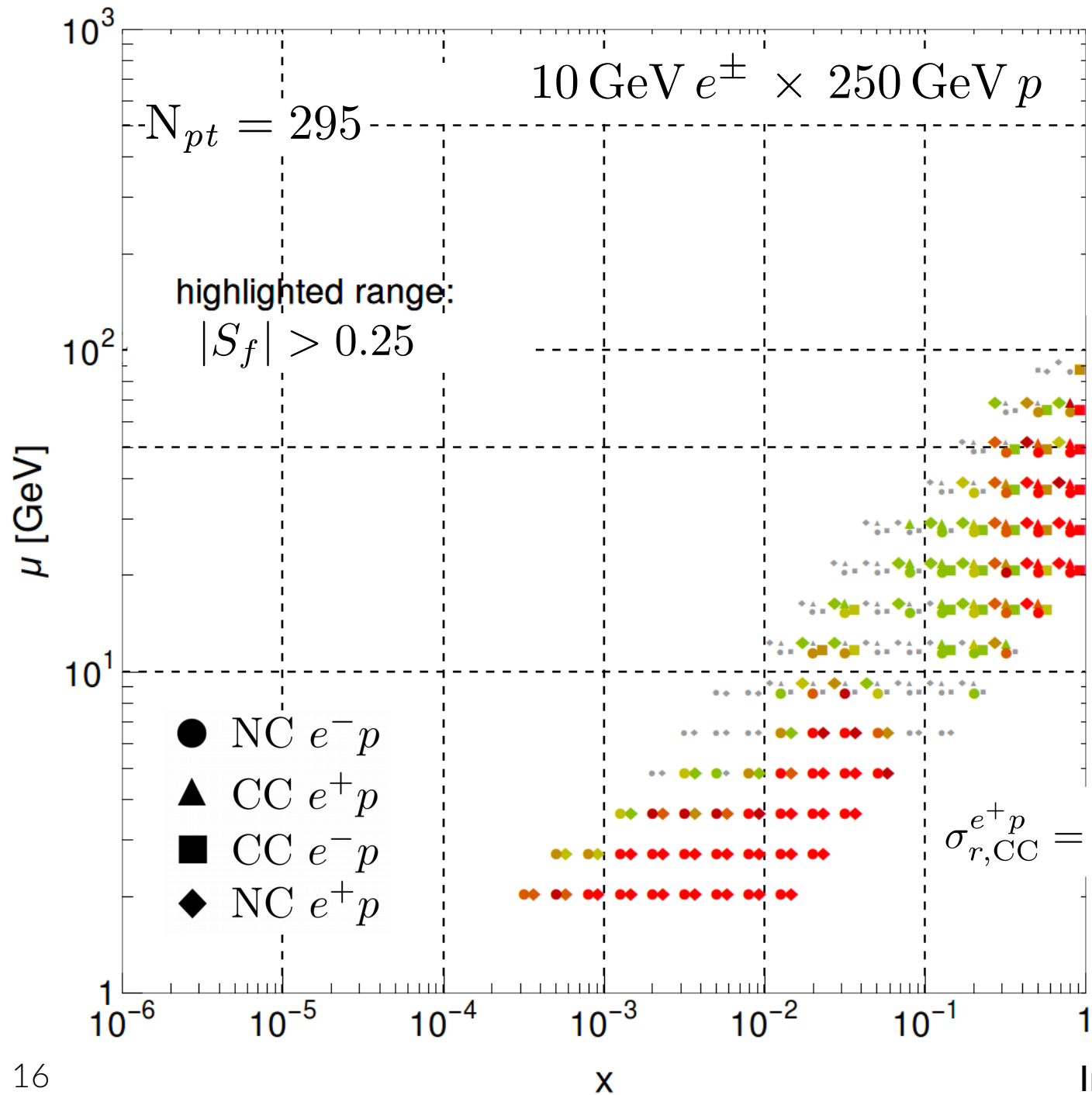
CJ15, Accardi et al., PRD93, 114017 (2016).



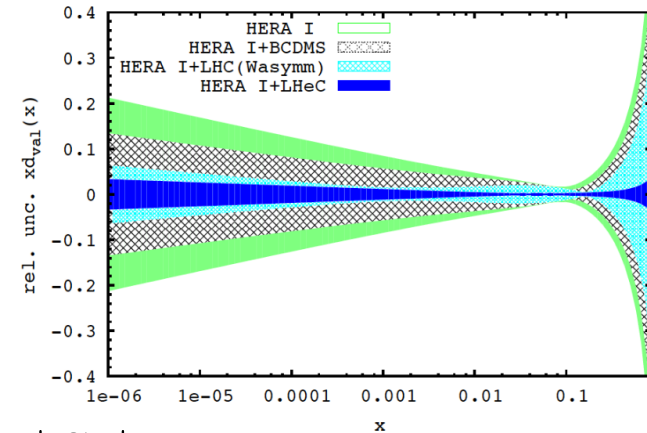
- BUT:** in the absence of a free neutron target, scattering from nuclei (e.g., the deuteron) is necessary

→ nuclear corrections (Fermi motion) are sizable, especially for large  $x$

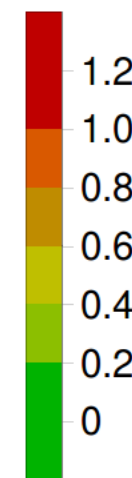
# $|S_f|$ for $d(x, \mu)$ CT14 HERA2 NNLO



EIC Whitepaper:1206.2913



$|S_f|$



- an EIC affords **strong sensitivities without a nuclear target**; here, at both very high and very low  $x$

for  $x \rightarrow 1$

$$\sigma_{r,CC}^{e^+p} = \frac{Y_+}{2} W_2^+ \mp \frac{Y_-}{2} x W_3^+ - \frac{y^2}{2} W_L^+ \simeq [1 - y]^2 x (d + s)$$

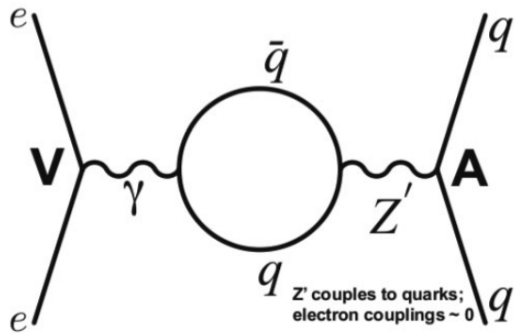
In the **LO quark-parton model**

# the electroweak sector and **New Physics** searches at EIC

- if measured to sufficient precision, the quark-level electroweak couplings may be sensitive to an extended EW sector, e.g.,  $Z'$

$$\mathcal{L}^{\text{PV}} = \frac{G_F}{\sqrt{2}} \left[ \bar{e} \gamma^\mu \gamma_5 e \left( C_{1u} \bar{u} \gamma_\mu u + C_{1d} \bar{d} \gamma_\mu d \right) + \bar{e} \gamma^\mu e \left( C_{2u} \bar{u} \gamma_\mu \gamma_5 u + C_{2d} \bar{d} \gamma_\mu \gamma_5 d \right) \right]$$

$$C_{1u} = -\frac{1}{2} + \frac{4}{3} \sin^2 \theta_W$$



- a unique strength of an EIC is its combination of very high precision and **beam polarization**, which allows the observation of **parity-violating helicity asymmetries**:

$$A^{\text{PV}} = \frac{\sigma_R - \sigma_L}{\sigma_R + \sigma_L} \quad (\text{R/L} : e^- \text{ beam helicities})$$

**selects  $\gamma$ - $Z'$  interference diagrams!**

TJH and Melnitchouk, PRD77, 114023 (2008).

$$A^{\text{PV}} = - \left( \frac{G_F Q^2}{4\sqrt{2}\pi\alpha} \right) (Y_1 a_1 + Y_3 a_3)$$

$$a_1 = \frac{2 \sum_q e_q C_{1q} (q + \bar{q})}{\sum_q e_q^2 (q + \bar{q})}$$

$$a_3 = \frac{2 \sum_q e_q C_{2q} (q - \bar{q})}{\sum_q e_q^2 (q + \bar{q})}$$

# the electroweak sector and **New Physics** searches at EIC

- if measured to sufficient precision, the quark-level electroweak couplings may be sensitive to an extended EW sector, e.g.,  $Z'$

$$\mathcal{L}^{\text{PV}} = \frac{G_F}{\sqrt{2}} \left[ \bar{e} \gamma^\mu \gamma_5 e \left( C_{1u} \bar{u} \gamma_\mu u + C_{1d} \bar{d} \gamma_\mu d \right) + \bar{e} \gamma^\mu e \left( C_{2u} \bar{u} \gamma_\mu \gamma_5 u + C_{2d} \bar{d} \gamma_\mu \gamma_5 d \right) \right]$$

$$C_{1u} = -\frac{1}{2} + \frac{4}{3} \sin^2 \theta_W$$

→ with sufficient precision, an EIC (which will be statistics-limited in these measurements) can extract  $\sin^2 \theta_W$

- this measurement is potentially sensitive to the TeV-scale in a complementary fashion to energy-frontier searches!

TJH and Melnitchouk, PRD77, 114023 (2008).

$$A^{\text{PV}} = - \left( \frac{G_F Q^2}{4\sqrt{2}\pi\alpha} \right) (Y_1 a_1 + Y_3 a_3)$$

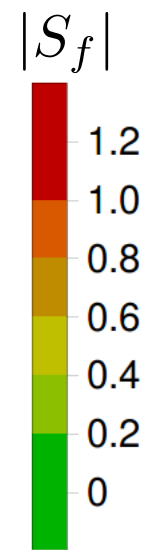
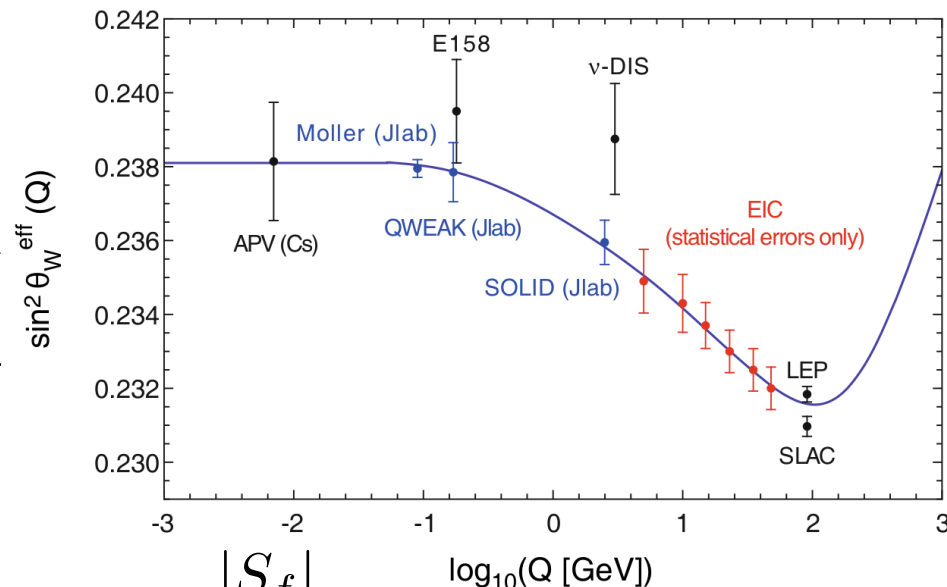
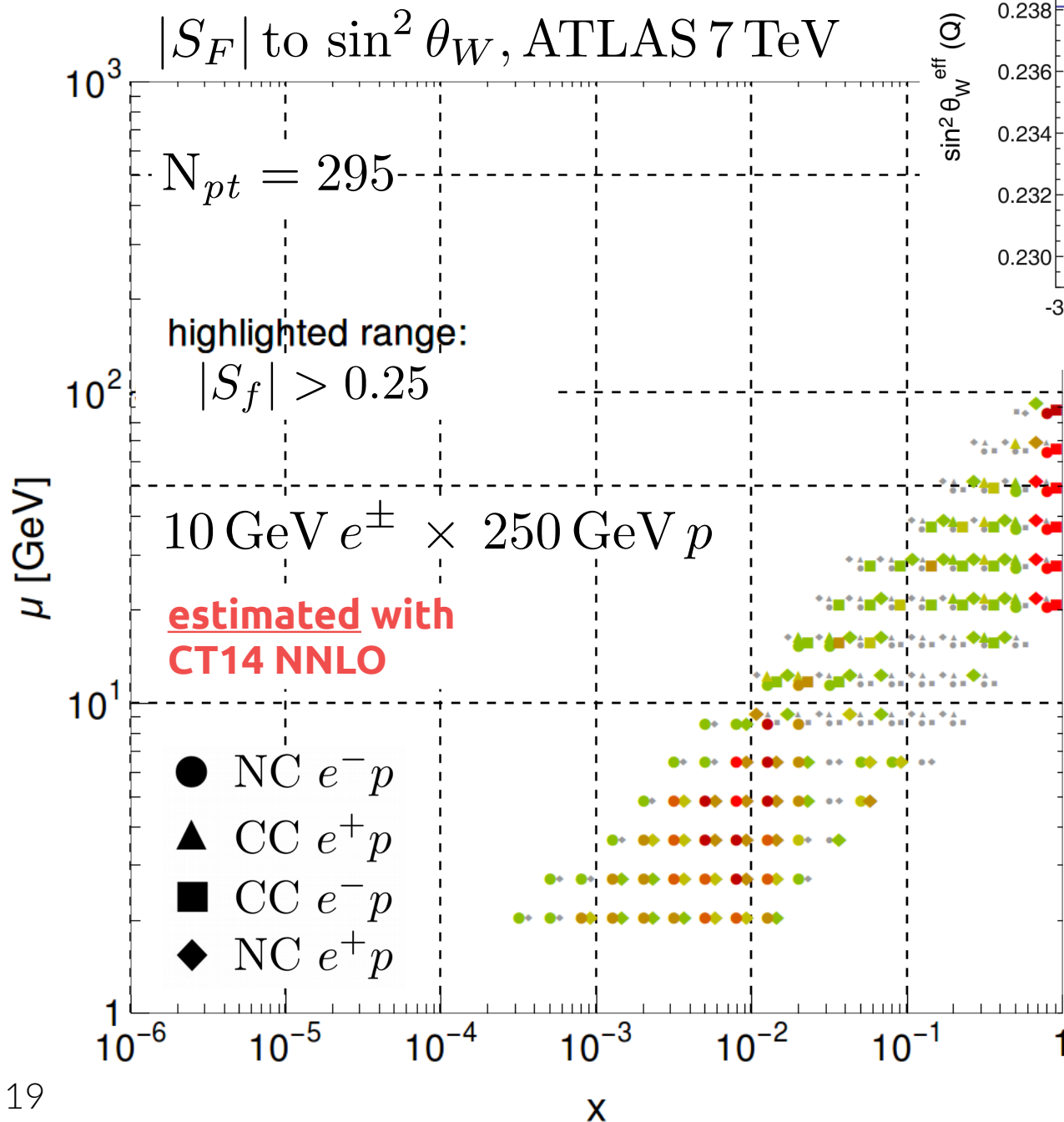
N.B.: extractions are dependent upon knowledge of the PDFs

$$a_1 = \frac{2 \sum_q e_q C_{1q} (q + \bar{q})}{\sum_q e_q^2 (q + \bar{q})}$$

$$a_3 = \frac{2 \sum_q e_q C_{2q} (q - \bar{q})}{\sum_q e_q^2 (q + \bar{q})}$$

# an EIC will probe EW parameters and New Physics!

Accardi et al., EPJA52, 268 (2016).



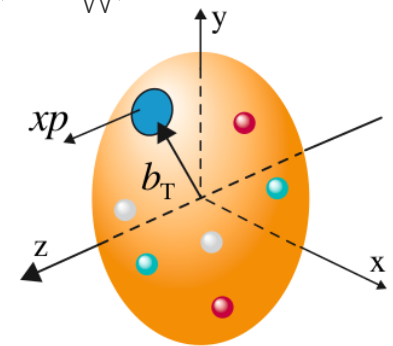
- observe a pronounced sensitivity to the Weinberg angle, especially low and high  $x$ , even at  $\mathcal{L} = 100\text{fb}^{-1}$
- this corresponds closely to the kinematics at which EIC is likely to measure  $A^{\text{PV}}$  — relatively large  $Q^2$  and in the  $x$  range  $0.2 \lesssim x \lesssim 0.5$



key points...

...and the future.

- numerous observables central to LHC's present/future discovery program at limited by uncertainties associated with nucleon structure
  - for the unpolarized PDFs, systematic tensions among modern world data are an impediment to higher precision for  $\sigma_H$ ,  $M_W$ , ...
  - an EIC will be ideally suited to perform measurements with the ability to unravel such systematic issues



### the EIC impact upon high-energy pheno will be pivotal

→ controlling PDFs/SM backgrounds; BSM searches; event generators

- confronting systematic PDF issues and exploring the HEP implications of the EIC require **community efforts**, esp. to optimize the output of the eventual program and its utility to HEP

many areas on both sides of the medium-, high-energy divide in which input is needed.



THANKS!!

**WE WANT YOU!**

—— supplementary material ——

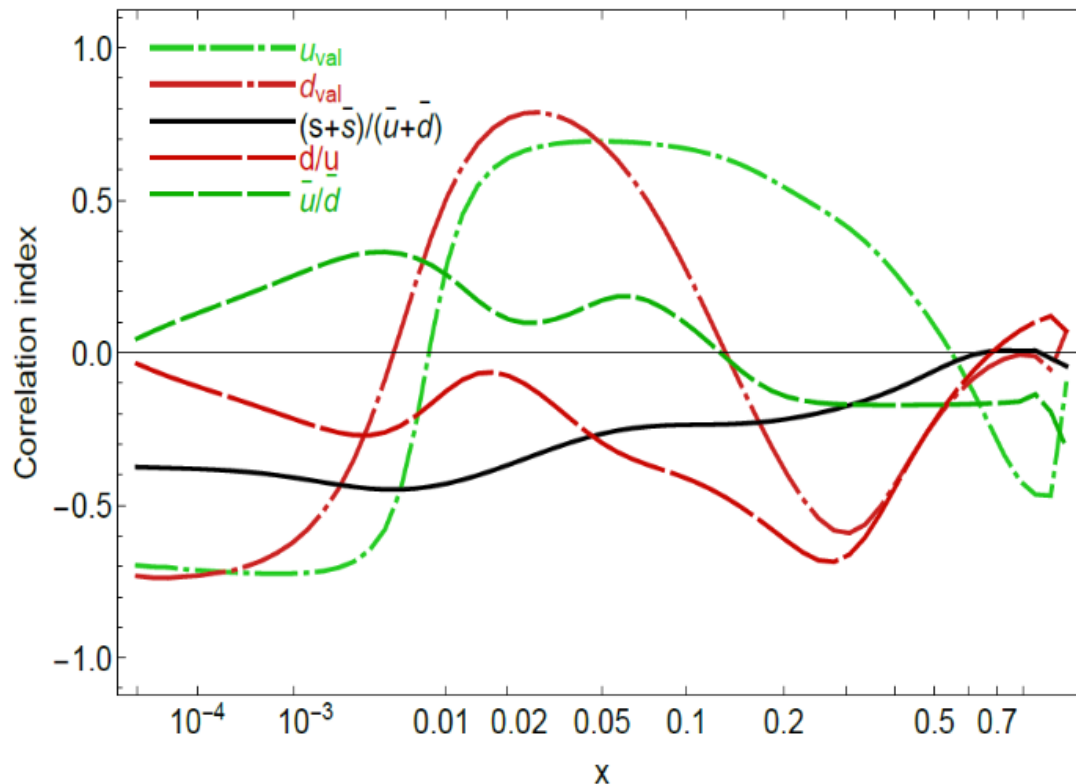
$\sin^2 \theta_W$  (and, eventually,  $M_W$ )

...as a follow-on to Alessandro's EW-focused overview:

important PDF correlations for the ATLAS extraction of  $\sin^2 \theta_W$

## Example: $\sin^2 \theta_{weak} \equiv s2w$ measured by ATLAS 8 TeV

Correlation,  $\sin^2 \theta_W$  (ATLAS 8 TeV CB) and  $f(x,Q)$  at  $Q=81.45$  GeV  
2018/11/11, PRELIMINARY, CT14 NNLO



Strongest correlations of  $s2w$  with  $u_{val}, d_{val}$  at  $0.005 \lesssim x \lesssim 0.2$

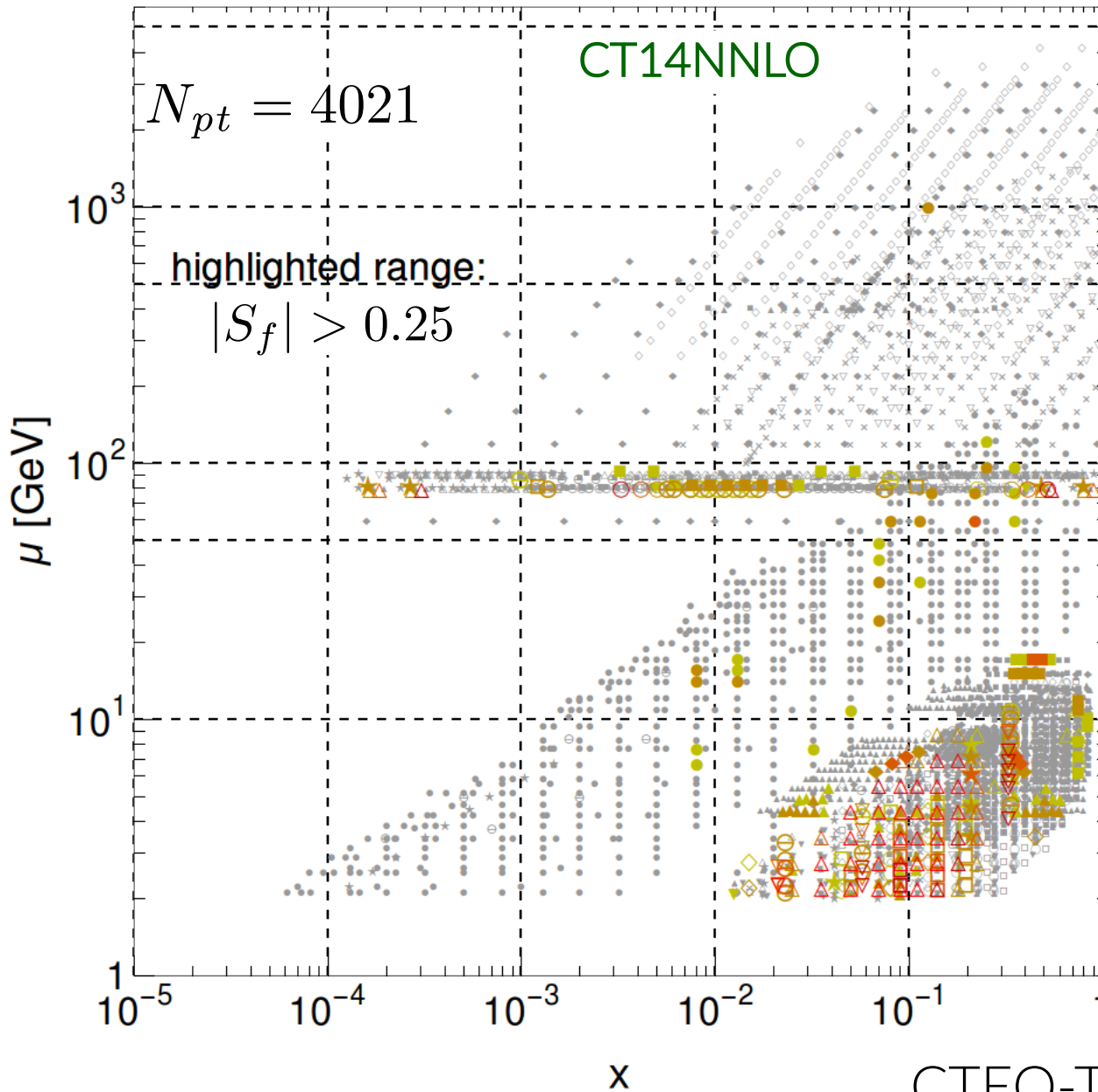
weak correlations with  $\bar{u}, \bar{d}, \bar{s}, g$

$u_{val}, d_{val}$  changed between CT10 and CT14 [1506.07433, Sec. 2B]

It is instructive to explore the data pulls on  $u_{val}, d_{val}$

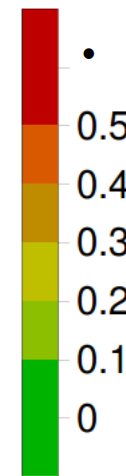
$$\sin^2 \theta_W$$

PDF sensitivity of  $\sin^2 \theta_W$  from 7 TeV ATLAS data



CTEQ-TEA sensitivities to  $\sin^2 \theta_W$

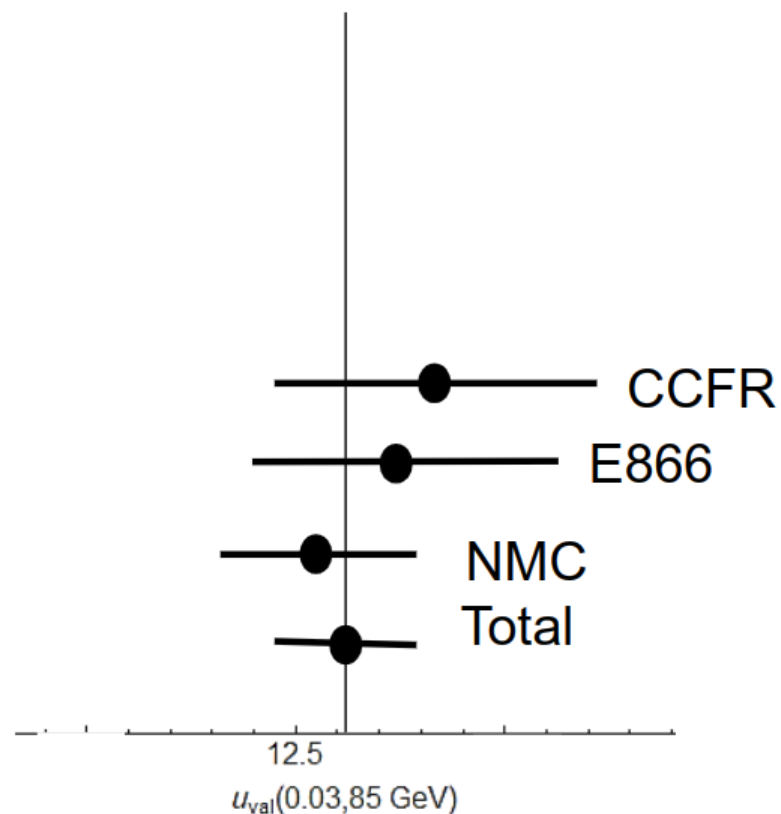
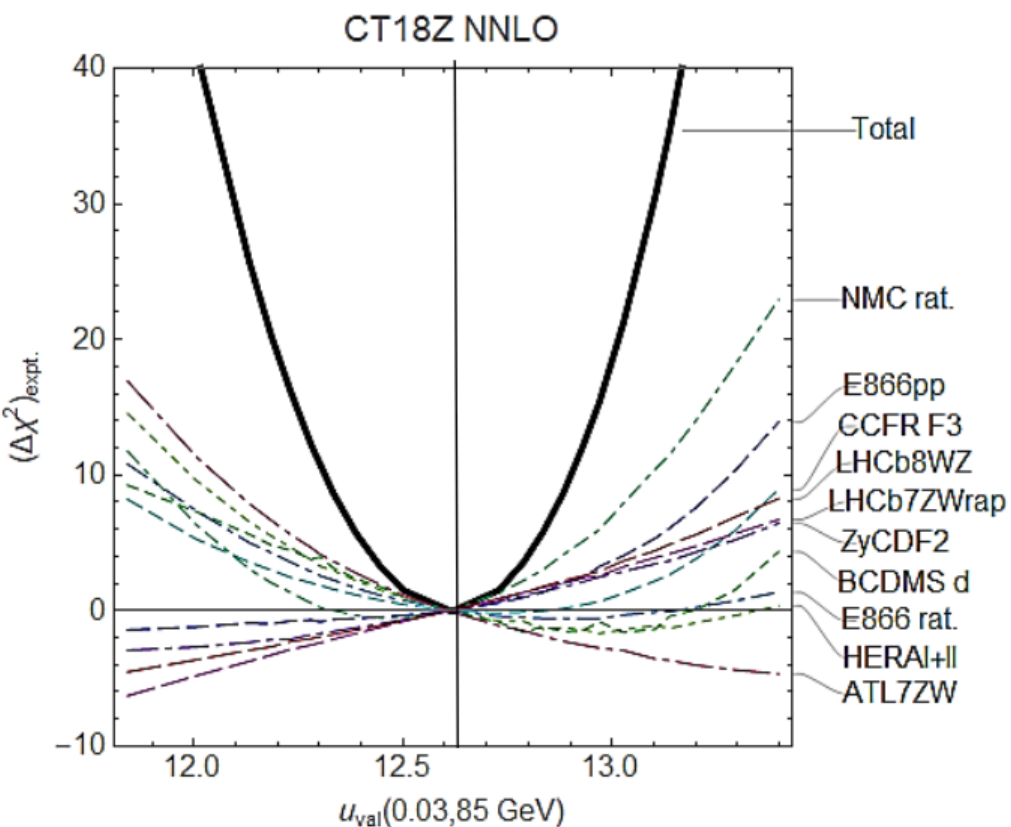
- **combined HERA1 DIS [most sensitive]**
- CCFR  $\nu p$  DIS  $F_{3,2}$
- BCDMS  $F_2^{p,d}$
- NMC  $ep, ed$  DIS
- CDHSW  $\nu A$  DIS
- NuTeV  $\nu A \rightarrow \mu\mu X$
- CCFR  $\nu A \rightarrow \mu\mu X$
- E866  $pp \rightarrow \ell^+ \ell^- X$
- ATLAS 7 TeV W/Z ( $35 \text{ pb}^{-1}$ )



... using a Lagrange Multiplier scan...

... or using residuals for replicas

[errors and correlations; most replicas are not good fits]



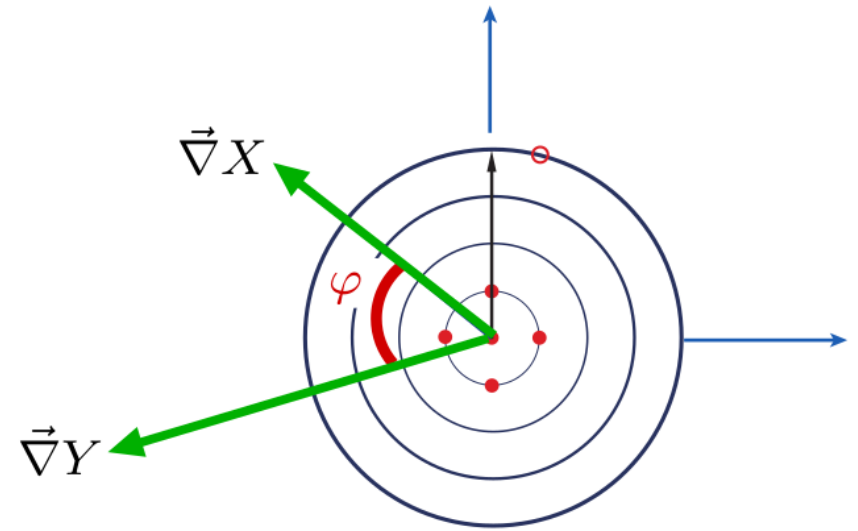
PRELIMINARY

Can repeat for  $s_2w$ ,  $M_W$ , ...



rather than the costly LM scans, we can examine a “cheaper” measure which yields comparable information

the  $L_2$  sensitivity



$L_2$  sensitivity. Take  $X = f_a(x_i, Q_i)$  or  $\sigma(f)$ ;  $Y = \chi_E^2$  for experiment  $E$ . Find  $\Delta Y(\vec{z}_{m,X})$  for the displacement  $|\vec{z}_{m,X}| = 1$  along the direction  $\vec{\nabla} X / |\vec{\nabla} X|$  (corresponding to  $\Delta \chi_{tot}^2 = T^2$  and  $X(\vec{z}) = X(0) + \Delta X$ ):

$$S_{f,L_2} \equiv \Delta Y(\vec{z}_{m,X}) = \vec{\nabla} Y \cdot \vec{z}_{m,X} = \vec{\nabla} Y \cdot \frac{\vec{\nabla} X}{|\vec{\nabla} X|}$$

$$= \Delta Y \cos \varphi$$

$$\text{or, } \sim \text{Corr}[f_a, \chi_E^2]$$

...extent to which total  $\chi_E^2$  of specific expts. correlates with  $x$ -dep. of PDFs

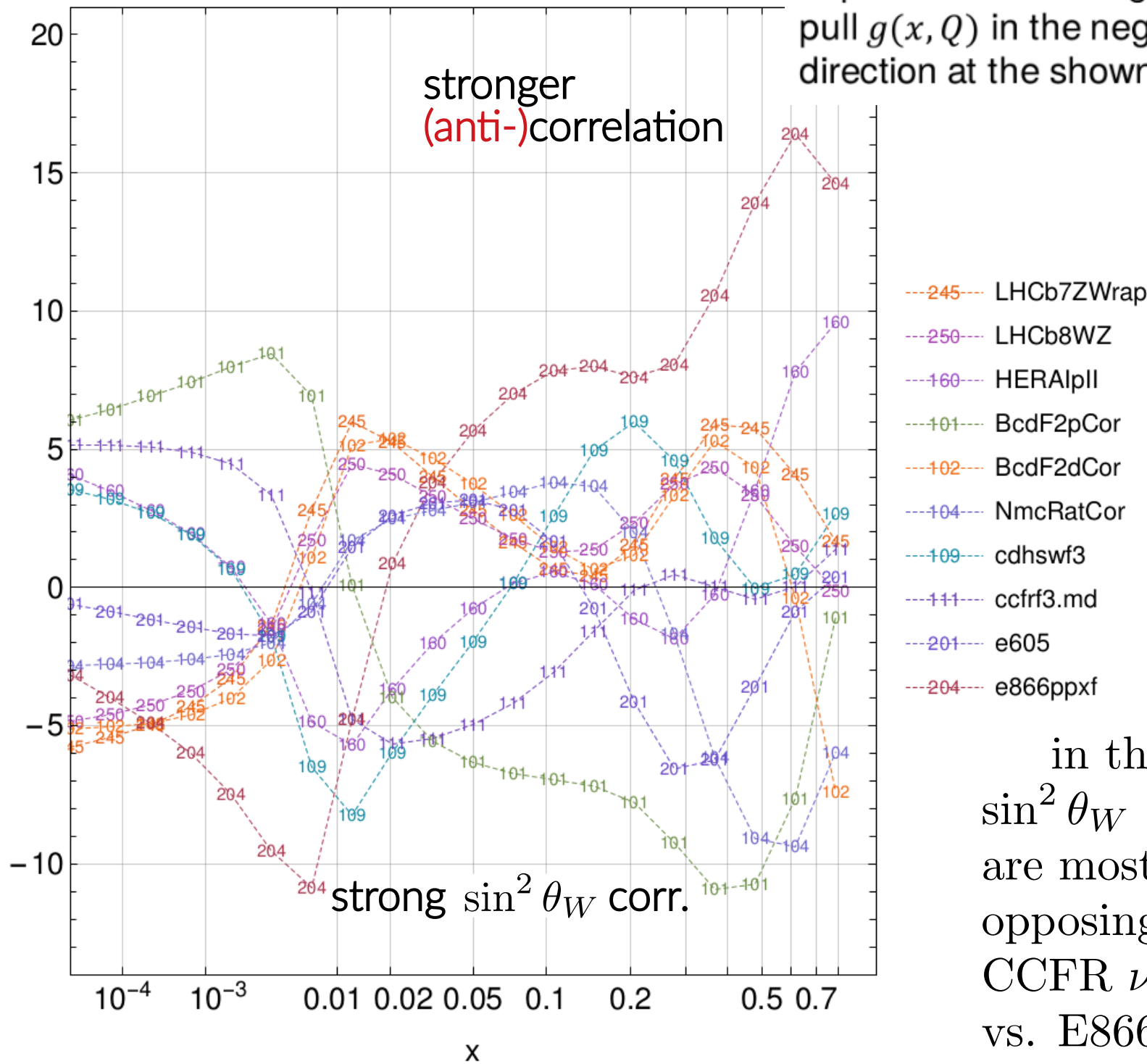
# CT18 NNLO, $u_V(x, Q)(x, 100 \text{ GeV})$

Experiments with large  $\Delta\chi^2 > 0$  [ $\Delta\chi^2 < 0$ ]  
pull  $g(x, Q)$  in the negative [positive]  
direction at the shown  $x$

stronger  
(anti-)correlation

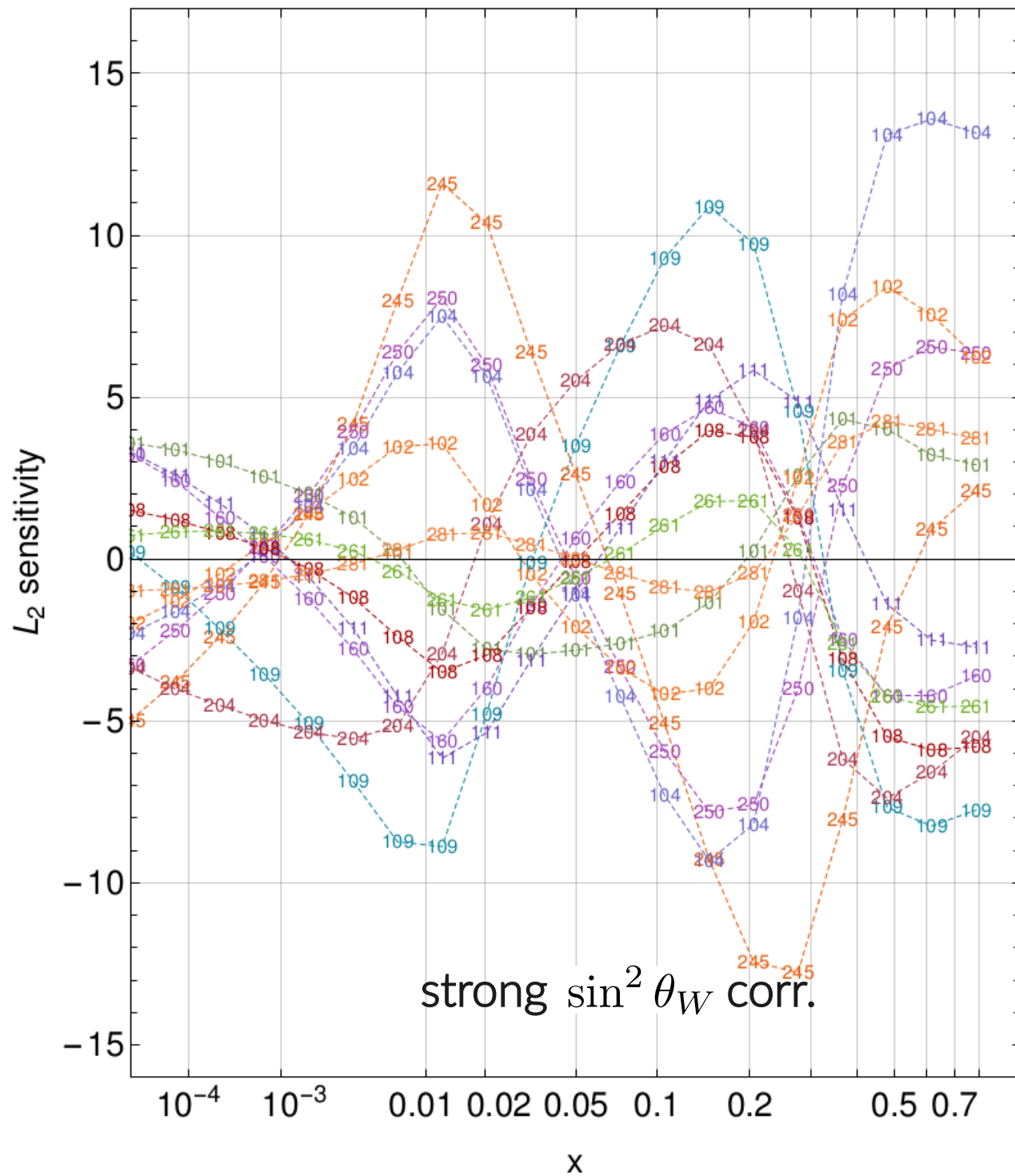
tension between  
LHCb W/Z  
data (245, 250);  
fixed-target DIS,  
Drell-Yan  
(CDHSW  $F_3$   
[109], E866pp  
[204])

$L_2$  sensitivity



in the region where  
 $\sin^2 \theta_W$  and  $u_v$   
are most correlated,  
opposing pulls from  
CCFR  $\nu$ DIS, BCDMS  
vs. E866  $pp$ , NMC rat.

# CT18 NNLO, $d_V(x, Q)(x, 100 \text{ GeV})$

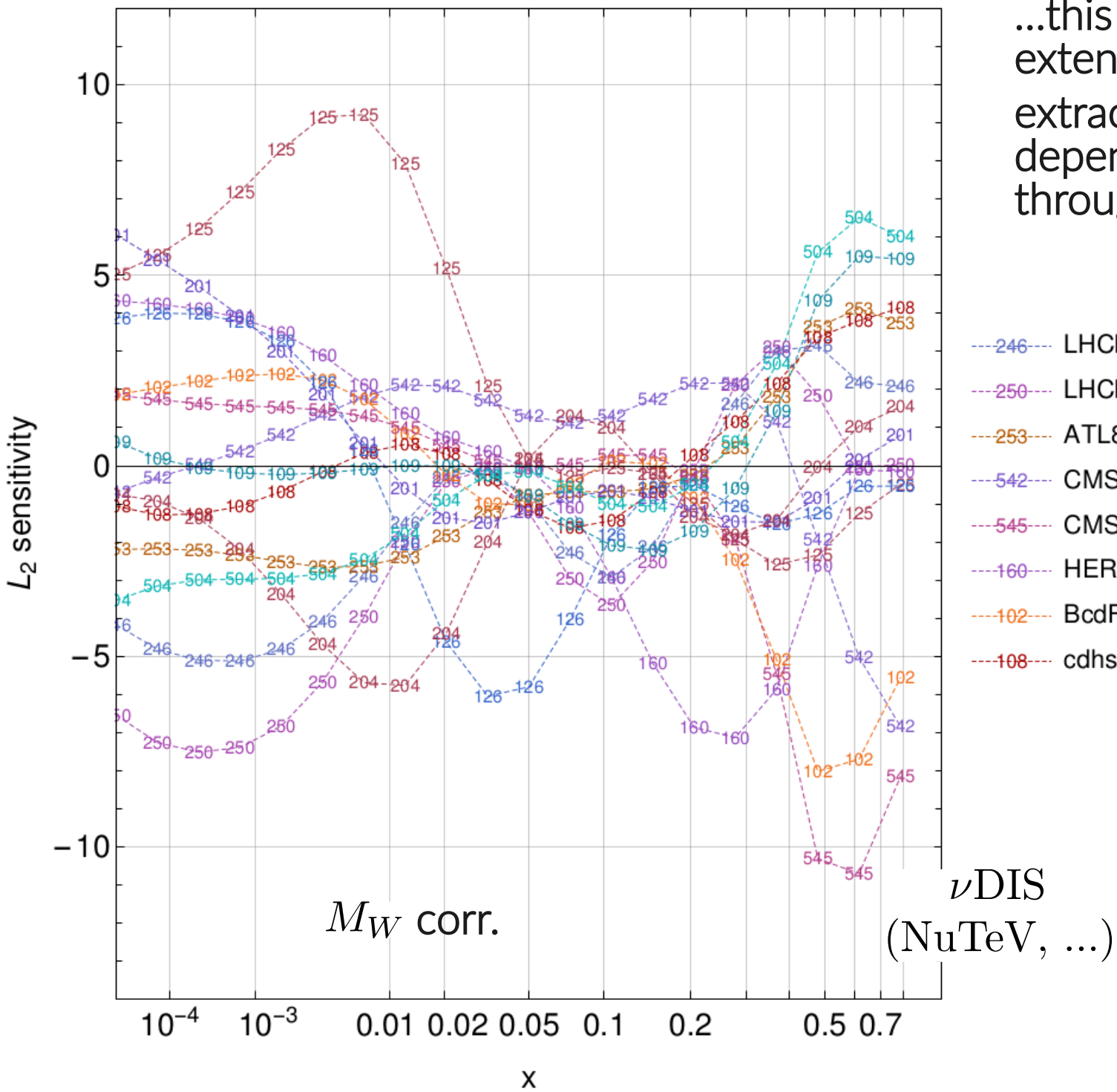


strong  $\sin^2 \theta_W$  corr.

tension between LHCb W/Z data (245, 250); fixed-target DIS, Drell-Yan (CDHSW  $F_3$  [109], E866pp [204])

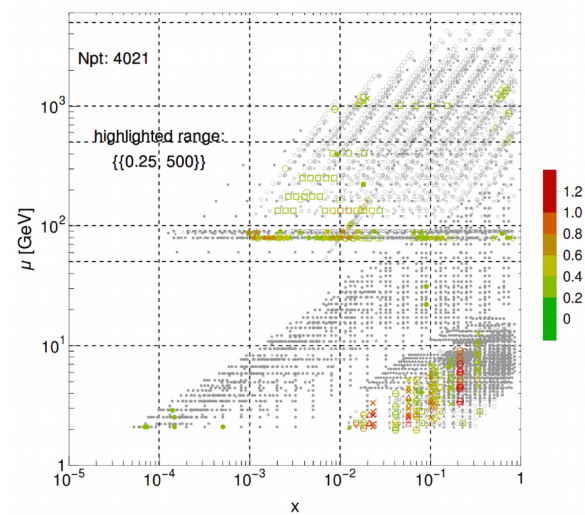
- 245--- LHCb7ZWrap
- 250--- LHCb8WZ
- 160--- HERA1pII
- 101--- BcdF2pCor
- 102--- BcdF2dCor
- 104--- NmcRatCor
- 108--- cdhswf2
- 109--- cdhswf3
- 111--- ccfrf3.md
- 204--- e866ppxf
- 261--- ZyCDF2
- 281--- d02Easy5

again, tensions observed between, e.g., NMC ratio data and CDHSW, E866pp

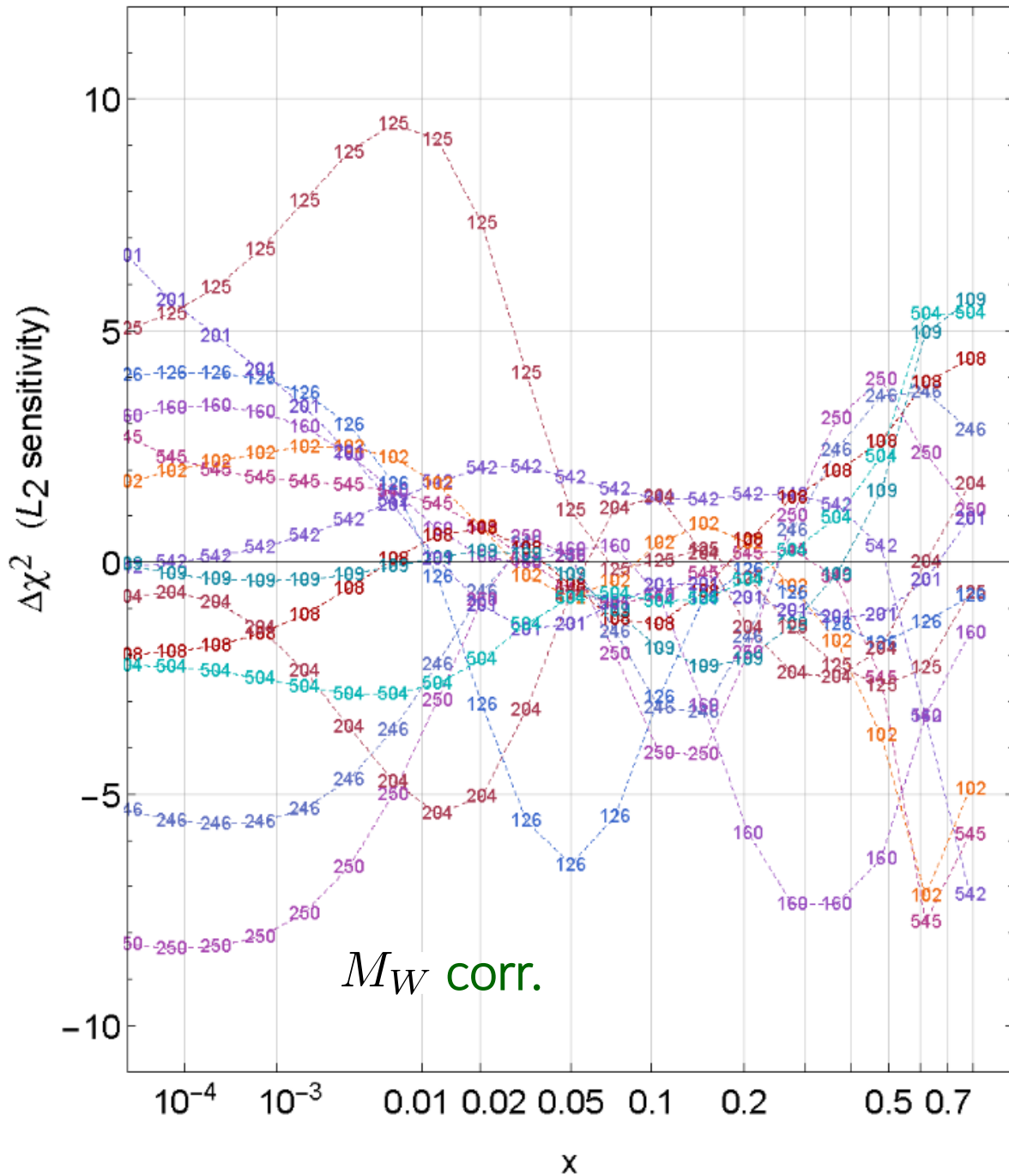
$M_W$ CT18 NNLO,  $s(x, 100 \text{ GeV})$ 

...this analysis can be extended to  $M_W$ ,  
 extractions of which are dependent upon  $s(x)$ ,  
 through Z-calibration

$|S_f|$  for  $s(x, \mu)$ , CT14HERA2NNLO



CT18 NNLO,  $s(x, 2 \text{ GeV})$



# $L_2$ sensitivity, strangeness: CT18

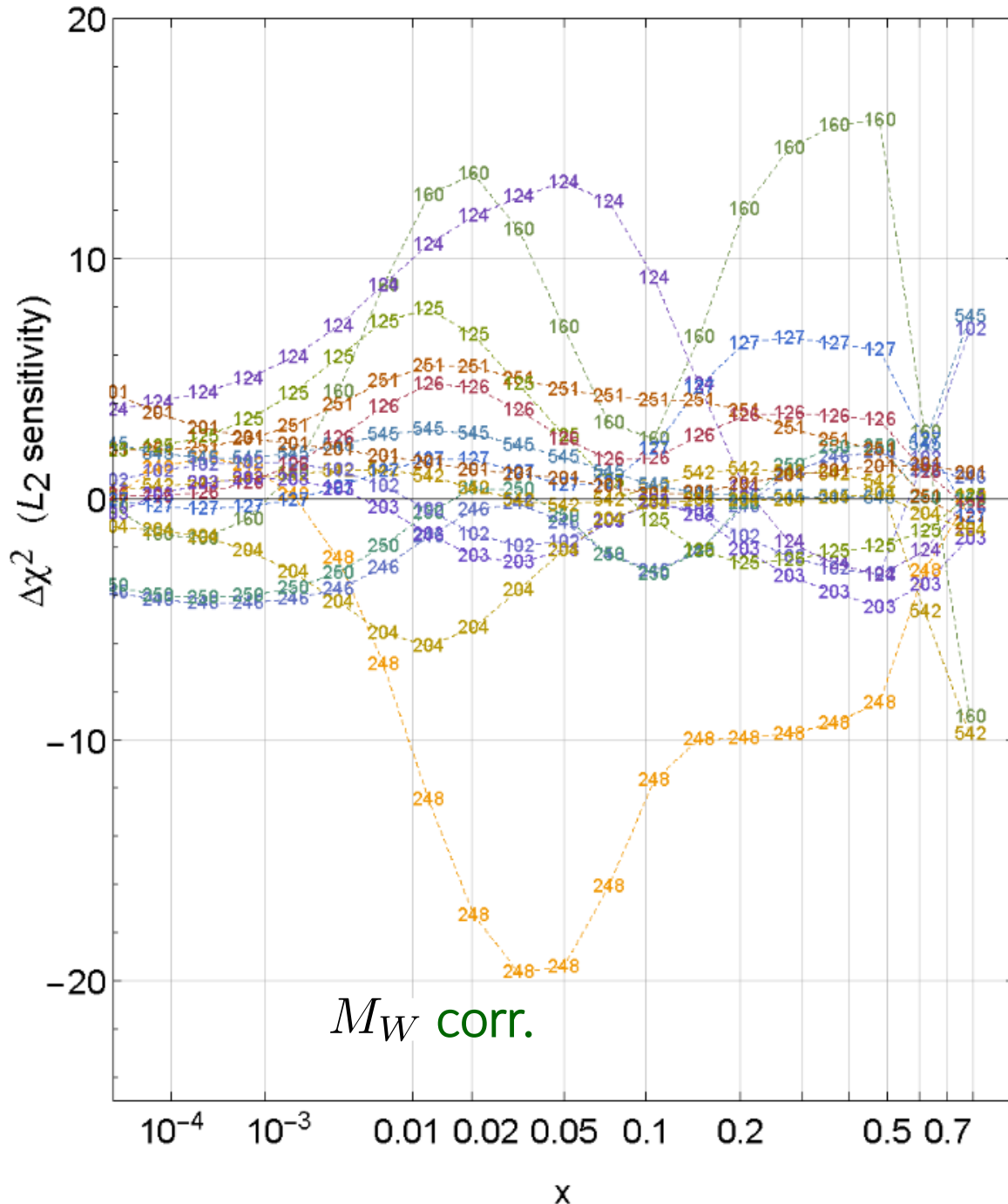
Most sensitive experiments

- 246--- LHCb8Zeer
- 250--- LHCb8WZ
- 542--- CMS7jtR7y6T
- 545--- CMS8jtR7T
- 160--- HERA I+II
- 102--- BcdF2dCor
- 108--- cdhswf2
- 109--- cdhswf3
- 125--- NuTeVChXN
- 126--- CcfrNuChXN
- 201--- e605
- 204--- e866ppxf
- 504--- cdf2jtCor2

A tension trend between DIS (HERA I+II, CCFR, NuTeV) and Drell-Yan (ATLAS 7 Z/W, LHCb W/Z, E866 pp, ...) experiments



CT18Z NNLO,  $s(x, 2 \text{ GeV})$



# $L_2$ sensitivity, strangeness: CT18Z

Most sensitive experiments

- 246--- LHCb8Zeer
- 248--- ATLAS7ZW.xF
- 250--- LHCb8WZ
- 251--- ATLAS8DY
- 542--- CMS7jtR7y6T
- 545--- CMS8jtR7T
- 160--- HERAII
- 102--- BcdF2dCor
- 124--- NuTeVNuChXN
- 125--- NuTeVNbChXN
- 126--- CcfrNuChXN
- 127--- CcfrNbChXN
- 201--- e605
- 203--- e866f
- 204--- e866ppxf

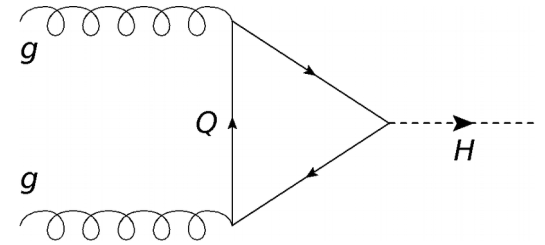
A tension trend between DIS (HERA I+II, CCFR, NuTeV) and Drell-Yan (ATLAS 7 Z/W, LHCb W/Z, E866 pp, ...) experiments

pronounced effect of ATLAS 7 TeV Z/W data!

# QCD at high energies: an EIC and control over the gluon

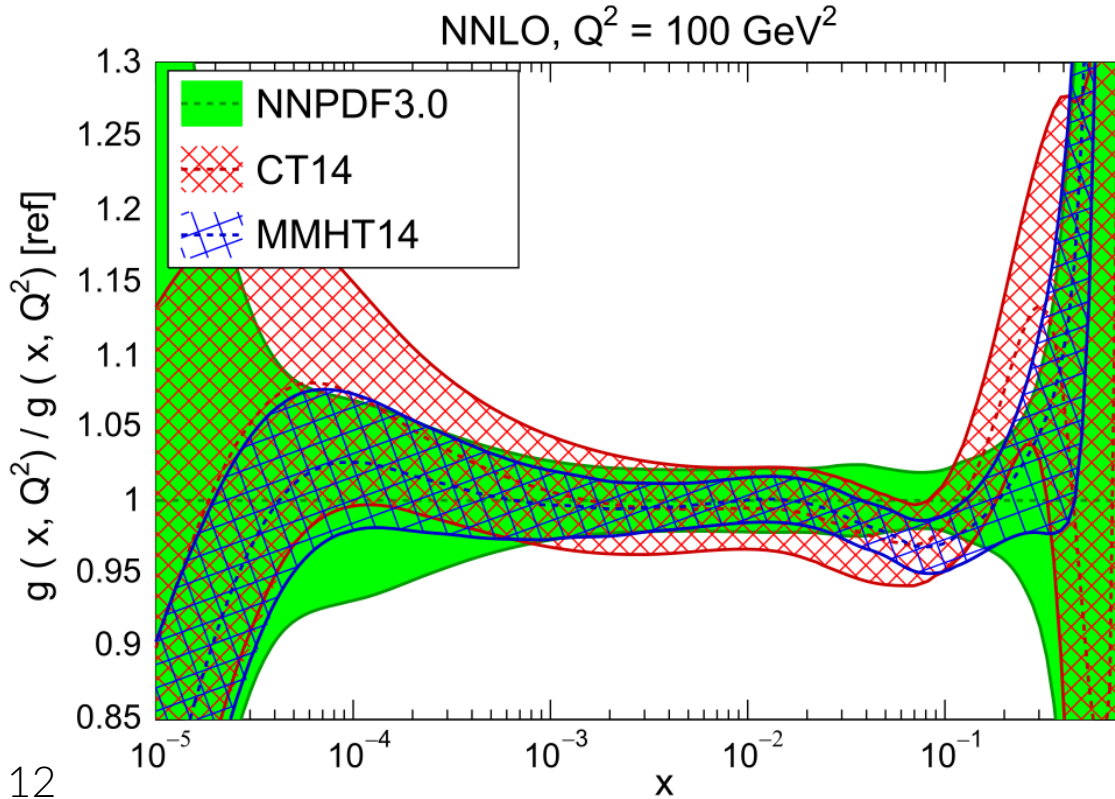
- the gluon is crucial to the mass of hadronic bound states, and  $gg \rightarrow H$  is the dominant channel in Higgs production

BUT

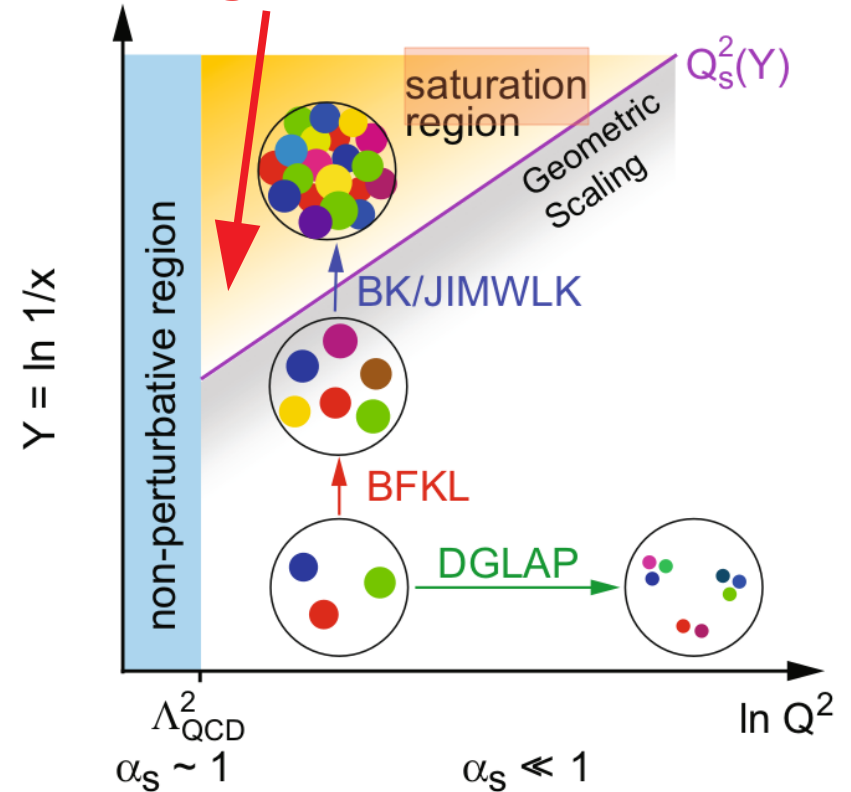


- while under better control at intermediate  $x$ , the collinear gluon PDF is poorly known toward the distribution endpoints, *i.e.*,  $g(x, \mu)$  for  $x \rightarrow 0, 1$

Rojo et al., J. Phys. G42, 103103 (2015).



can we begin to observe this transition?





the goal is to quantify the strength of the constraints placed on a particular set of PDFs by both individual and aggregated measurements *without direct fitting*

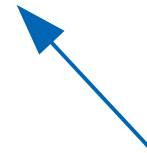
- for single-particle hadroproduction of gauge bosons at, e.g., LHC, factorization gives

$$\sigma(AB \rightarrow W/Z+X) = \sum_n \alpha_s^n(\mu_R^2) \sum_{a,b} \int dx_a dx_b$$

$$\times f_{a/A}(x_a, \mu^2) \hat{\sigma}_{ab \rightarrow W/Z+X}^{(n)}(\hat{s}, \mu^2, \mu_R^2) f_{b/B}(x_b, \mu^2)$$



PDFs determined by fits to data; e.g., "CT14H2"



pQCD matrix elements – specified by theoretical formalism in a given fit

- *idea*: study the statistical correlation between PDFs and the quality of the fit at a measured data point(s); fit quality encoded in a (Theory) – (shifted Data) *residual*:

$$r_i(\vec{a}) = \frac{1}{s_i} (T_i(\vec{a}) - D_{i,sh}(\vec{a}))$$

$s_i$  : uncorrelated uncert.

$\vec{a}$  : PDF parameters

# a brief statistical aside, i

- the CTEQ-TEA global analysis relies on the Hessian formalism for its error treatment

$$\chi_E^2(\vec{a}) = \sum_{i=1}^{N_{pt}} r_i^2(\vec{a}) + \sum_{\alpha=1}^{N_\lambda} \bar{\lambda}_\alpha^2(\vec{a})$$

← nuisance parameters to handle correlated errors

$$r_i(\vec{a}) = \frac{1}{s_i} (T_i(\vec{a}) - D_{i,sh}(\vec{a}))$$

these result in systematic shifts to data central values:

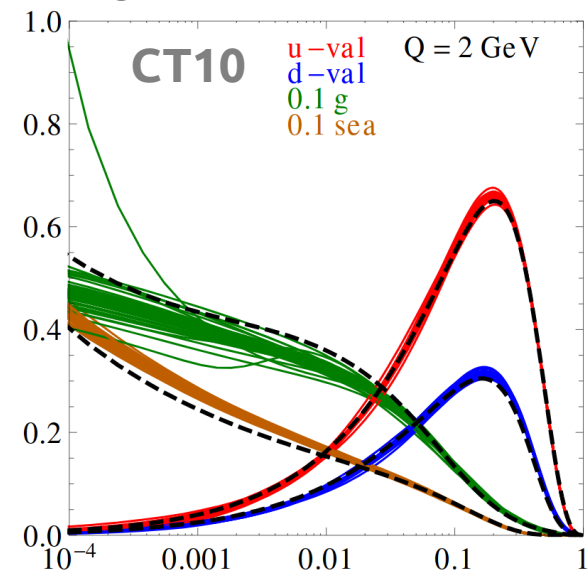
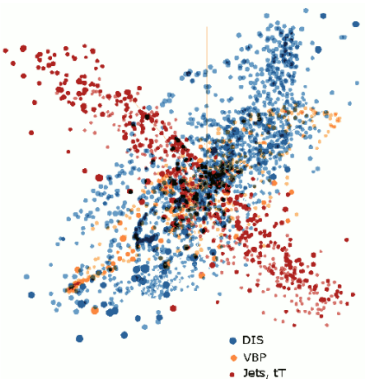
$$D_i \rightarrow D_{i,sh}(\vec{a}) = D_i - \sum_{\alpha=1}^{N_\lambda} \beta_{i\alpha} \bar{\lambda}_\alpha(\vec{a})$$

- a 56-dimensional parametric basis  $\vec{a}$  is obtained by diagonalizing the Hessian matrix H determined from  $\chi^2$  (following a 28-parameter fit)

**use this basis to compute 56-component "normalized" residuals:**

$$\delta_{i,l}^\pm \equiv (r_i(\vec{a}_l^\pm) - r_i(\vec{a}_0)) / \langle r_0 \rangle_E$$

where  $\langle r_0 \rangle_E \equiv \sqrt{\frac{1}{N_{pt}} \sum_{i=1}^{N_{pt}} r_i^2(\vec{a}_0)}$

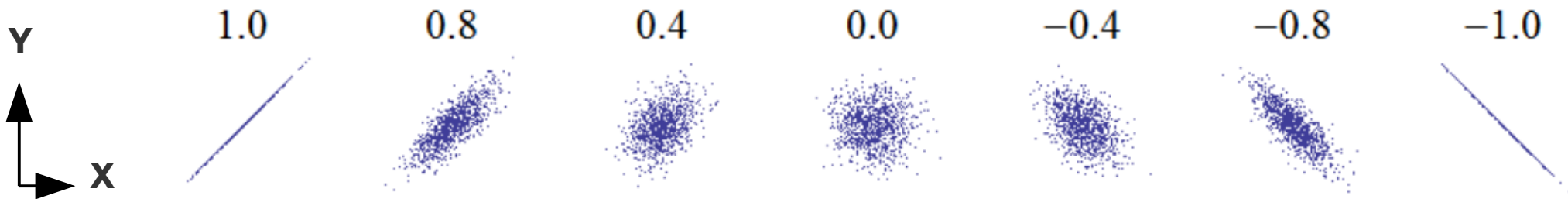


## a brief statistical aside, ii

- ... but how does the behavior of these residuals relate to the fitted PDFs and their uncertainties?

for example, how does the PDF uncertainty (at specific  $x, \mu$ ) correlate with the residual associated with a theoretical prediction at the same  $x, \mu$ ?

**examine the Pearson correlation over the 56-member PDF error set between a PDF of given flavor and the residual**



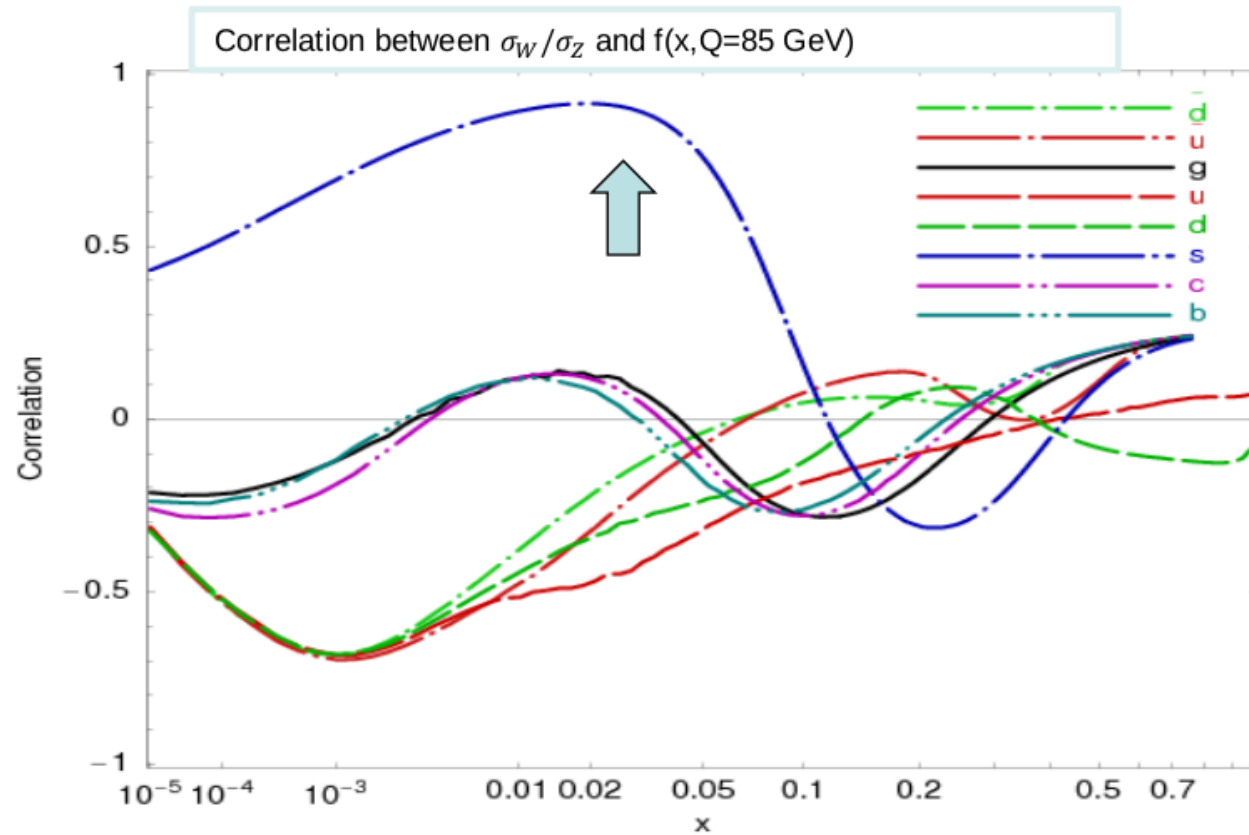
[X,Y] are exactly (anti-)correlated at the far (right) left above.

- we may then evaluate correlations between arbitrary PDF-derived quantities over the ensemble of error sets ([X,Y] may be PDFs, cross sections, residuals,...):

$$\text{Corr}[X, Y] = \frac{1}{4\Delta X \Delta Y} \sum_{j=1}^N (X_j^+ - X_j^-)(Y_j^+ - Y_j^-) \quad \Delta X = \frac{1}{2} \sqrt{\sum_{j=1}^N (X_j^+ - X_j^-)^2}$$

...we may turn to the Pearson correlations between PDFs and  $\delta_i$ , but we first note

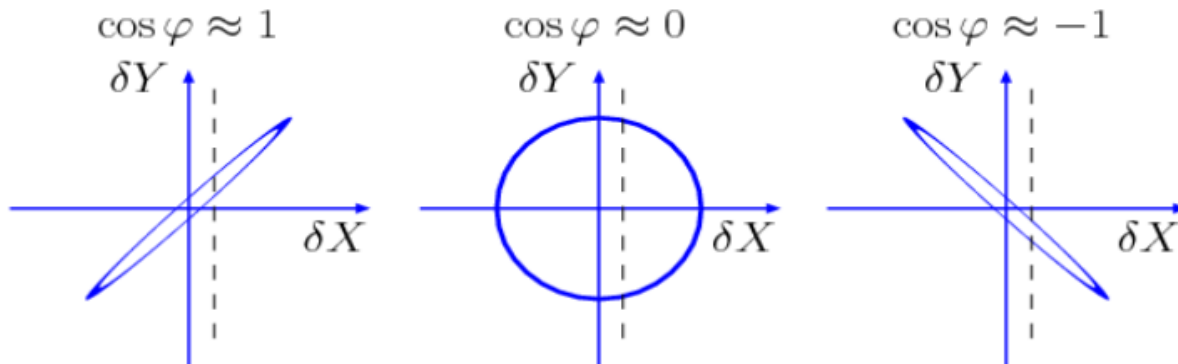
## Correlations carry useful, but limited information



**CTEQ6.6 [arXiv:0802.0007]:**

$\cos \varphi > 0.7$  shows that the ratio  $\sigma_W/\sigma_Z$  at the LHC must be sensitive to the strange PDF  $s(x, Q)$

$\cos \varphi \approx \pm 1$  suggests that a measurement of  $X$  **may** impose tight constraints on  $Y$



But,  $\text{Corr}[X, Y]$  between **theory** cross sections  $X$  and  $Y$  does not tell us about **experimental** uncertainties

# Correlation $C_f$ and sensitivity $S_f$

The relation of data point  $i$  on the PDF dependence of  $f$  can be estimated by:

- $C_f \equiv \text{Corr}[\rho_i(\vec{a}), f(\vec{a})] = \cos\varphi$

$\vec{\rho}_i \equiv \vec{\nabla}r_i / \langle r_0 \rangle_E$  -- gradient of  $r_i$  normalized to the r.m.s. average residual in expt E;

$$(\vec{\nabla}r_i)_k = (r_i(\vec{a}_k^+) - r_i(\vec{a}_k^-))/2$$

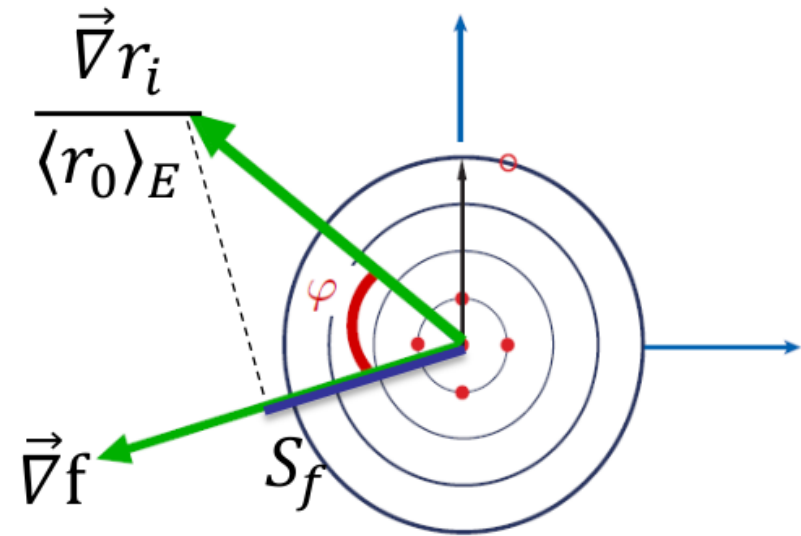
$$\text{Corr}[X, Y] = \frac{1}{4\Delta X \Delta Y} \sum_{j=1}^N (X_j^+ - X_j^-)(Y_j^+ - Y_j^-)$$

$C_f$  is **independent** of the experimental and PDF uncertainties. In the figures, take  $|C_f| \gtrsim 0.7$  to indicate a large correlation.

- $S_f \equiv |\vec{\rho}_i| \cos\varphi = C_f \frac{\Delta r_i}{\langle r_0 \rangle_E}$  -- projection of  $\vec{\rho}_i(\vec{a})$  on  $\vec{\nabla}f$

$S_f$  is proportional to  $\cos\varphi$  and the ratio of the PDF uncertainty to the experimental uncertainty. We can sum  $|S_f|$ .

In the figures, take  $|S_f| > 0.25$  to be significant.



## 2<sup>nd</sup> aside: kinematical matchings

- residual-PDF correlations and sensitivities are evaluated at parton-level kinematics determined according to leading-order matchings with physical scales in measurements

deeply-inelastic scattering:

$$\mu_i \approx Q|_i, \quad x_i \approx x_B|_i$$

$x_i$  : parton mom. fraction

$\mu_i$  : factorization scale

hadron-hadron collisions:

$AB \rightarrow CX$

$$\mu_i \approx Q|_i, \quad x_i^\pm \approx \frac{Q}{\sqrt{s}} \exp(\pm y_C)|_i$$

single-inclusive jet production:

$$Q = 2p_{Tj}, \quad y_C = y_j$$

$t\bar{t}$  pair production:

$$Q = m_{t\bar{t}}, \quad y_C = y_{t\bar{t}}$$

etc...

$d\sigma/dp_T^Z$  measurements:

$$Q = \sqrt{(p_T^Z)^2 + (M_Z)^2}, \quad y_C = y_Z$$

# Sensitivity ranking tables

... to assess the impact of separate experiments

No.	Expt.	$N_{pt}$	Rankings, <b>CT14 HERA2 NNLO PDFs</b>												
			$\sum_f  S_f^E $	$\langle \sum_f  S_f^E  \rangle$	$ S_{\bar{d}}^E $	$\langle  S_{\bar{d}}^E  \rangle$	$ S_{\bar{u}}^E $	$\langle  S_{\bar{u}}^E  \rangle$	$ S_g^E $	$\langle  S_g^E  \rangle$	$ S_u^E $	$\langle  S_u^E  \rangle$	$ S_d^E $	$\langle  S_d^E  \rangle$	$ S_s^E $
1	HERAI+II'15	1120.	620.	0.0922	B		<b>A</b>	3	<b>A</b>	3	<b>A</b>	3	B		C
2	CCFR-F3'97	86	218.	0.423	C	<b>1</b>	C	<b>1</b>		3	B	<b>1</b>	C	2	
3	BCDMSp'89	337	184.	0.0908					C		B	3	C		
4	NMCrat'97	123	169.	0.229	C	2					C	2	B	2	
5	BCDMSd'90	250	141.	0.0939	C				C	3	C	3	C	3	
6	CDHSW-F3'91	96	115.	0.199	C	2	C	2		3	C	2	C	3	
7	E605'91	119	113.	0.158	C	2	C	2				3			
8	E866pp'03	184	103.	0.0935		3	C	3			C	3			
9	CCFR-F2'01	69	89.1	0.215		3		3	C	2		3		2	3
10	<b>CMS8jets'17</b>	185	87.6	0.0789					C	3					
11	CDHSW-F2'91	85	82.4	0.162		3		3		3		3	C	3	
12	CMS7jets'13	133	63.8	0.0799					C	3					
13	NuTeV-nu'06	38	58.9	0.259		3		3				3		3	C <b>1</b>
14	<b>CMS7jets'14</b>	158	57.5	0.0606					C	3					
15	CCFR SI nub'01	38	49.4	0.217		3		3				3		3	C <b>1</b>
16	<b>ATLAS7jets'15</b>	140	48.2	0.0574						3					
17	CCFR SI nu'01	40	48.	0.2		3		3				3		3	C <b>1</b>

Experiments are listed in the descending order of the summed sensitivities to  $\bar{d}, \bar{u}, g, u, d, s$

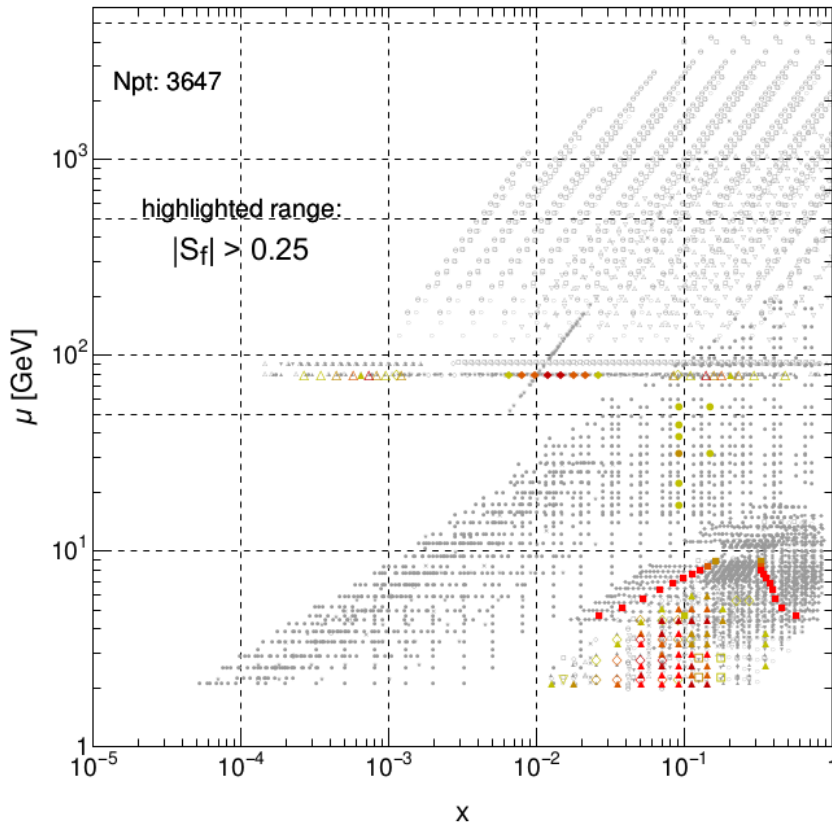
For each flavor, A and 1 indicate the strongest total sensitivity and strongest sensitivity per point

C and 3 indicate marginal sensitivities; low sensitivities are not shown

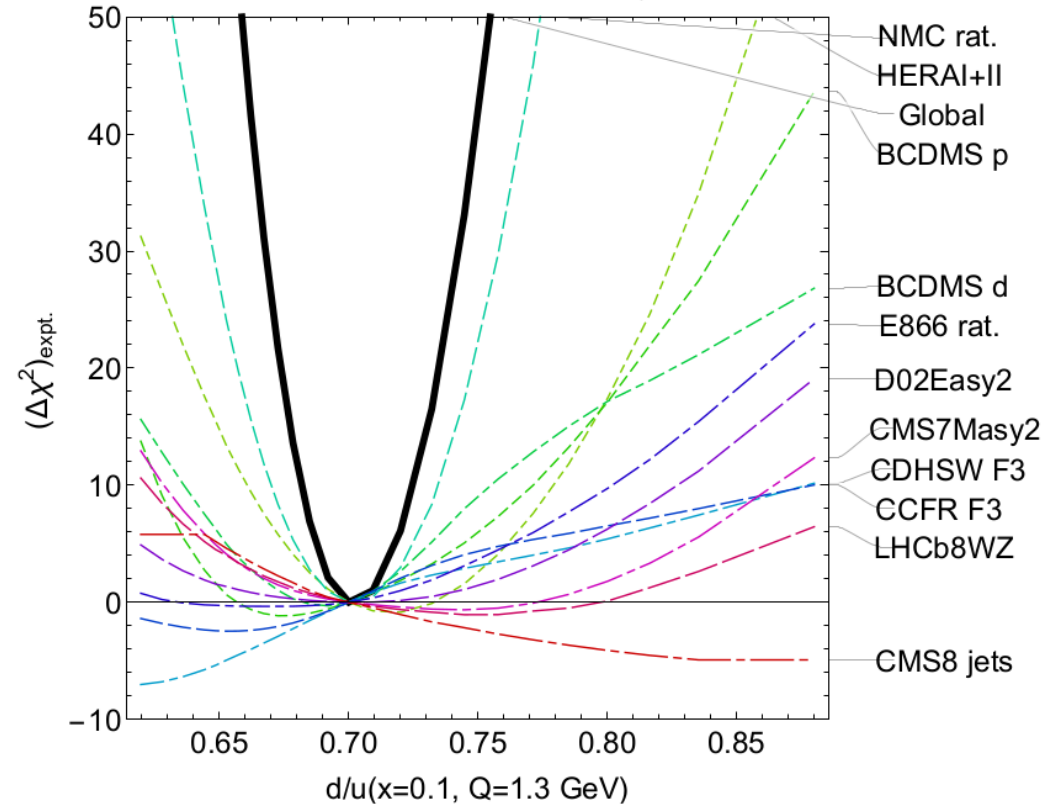


# PDFSense predictions can be validated against actual fits

$|S_f|$  for  $d/u(0.1,1.3)$ , CT18pre NNLO



CT18 NNLO, + 0.5% theory error



- PDFSense successfully predicts the highest impact data sets *before* fitting, as shown in this illustration for the large  $x$  PDF ratio  $d/u$
- Lagrange Multiplier scans provide an independent test of which datasets most drive the global fit in connection with specific PDFs

**HERA and fixed-target (BCDMS, NMC) data are dominant!**